

# ANN-based Automated Scaffold Builder Activity Recognition through Wearable EMG and IMU Sensors

Srikanth Sagar Bangaru<sup>1</sup>, Chao Wang<sup>2\*</sup>, Sri Aditya Busam<sup>3</sup>, and Fereydoun Aghazadeh<sup>4</sup>

4     <sup>1</sup>Ph.D. Candidate, Intelligent Construction Management Lab (ICML), Bert S. Turner Department  
5      of Construction Management, Louisiana State University, 237 Electrical Engineering Building,  
6      Baton Rouge, LA 70803; PH: (405) 762-3689; email: sbanga3@lsu.edu

7     <sup>2</sup>Assistant Professor, Intelligent Construction Management Lab (ICML), Bert S. Turner  
8     Department of Construction Management, Louisiana State University, 3315D Patrick F. Taylor  
9     Hall, Baton Rouge, LA 70803; PH (225) 578-9175; email: [chaowang@lsu.edu](mailto:chaowang@lsu.edu)

10 <sup>3</sup>Master Student, Department of Mechanical & Industrial Engineering, Louisiana State University,  
11 Patrick F. Taylor Hall, Baton Rouge, LA 70803; PH: (225) 288-6287; email: sbusam1@lsu.edu

12     <sup>4</sup>Professor, Department of Mechanical & Industrial Engineering, Louisiana State University,  
13     3250A Patrick F. Taylor Hall, Baton Rouge, LA 70803; PH (225) 578-5367; email:  
14     aghazadeh@lsu.edu

15 \*Correspondence: chaowang@lsu.edu; Tel.: +1-225-578-9175

## Abstract

17 Construction worker activity recognition is essential for worker performance and safety  
18 assessment. With the development of wearable sensing technologies, many researchers developed  
19 kinematic sensor-based worker activity recognition methods with considerable accuracy.  
20 However, the limitations of the previous studies remain at the challenge of using smartphones for  
21 practical implementation, fewer classified activities, and limited recognized motions and body  
22 parts. This study proposes an ANN-based automated construction worker activity recognition  
23 method that can recognize complex construction activities. The proposed methodology discusses  
24 data acquisition, data fusion, and artificial neural network (ANN) model development. A case  
25 study of scaffold builder activities was investigated to validate the proposed methodology's  
26 feasibility and evaluate its performance compared to other existing methods. The results show that  
27 the proposed model can recognize fifteen scaffold builder activities with an accuracy of 94% with  
28 0.94 weighted precision, recall, and F1 Score.

30

31 **Keywords: Artificial Neural Network, Wearable sensors, EMG, IMU, Activity recognition,**  
32 **Data fusion, Construction Worker, Scaffold Builder**

33

34 **1. Introduction**

35 The US construction industry is one of the world's largest markets, with annual expenditures  
36 of over \$1,293 billion and seven million employees [1]. However, the construction industry is  
37 facing a massive skilled workforce shortage [2]. More than 80% of the construction companies  
38 have reported that they have a hard time finding skilled craft workers. It is estimated that more  
39 than one million craft professionals are required by 2023, which includes various crafts such as  
40 carpentry, masonry, electricians, pipefitters, ironworkers, and scaffold builders, etc. [3]. In  
41 particular, the demand for craft professionals is very high in the US Gulf Coast area, with an  
42 increase in petrochemical investments [3]. As a result of workforce shortage, there is a significant  
43 impact on the project outcomes and worker performance, such as delayed project completion, an  
44 increase in overall project cost, and an increase in workload for the existing skilled workers [4].

45 One of the primary reasons for the workforce shortage in the construction industry is the premature  
46 retirement of the experienced, skilled workforce due to safety and health issues [5]. The  
47 Construction Industry Institute (CCI) and the Center for Construction Research and Training  
48 (CPWR) have established various training programs and investigated various new technologies to  
49 improve construction safety and health [6]. Various researchers have proposed different  
50 technology-based solutions to prevent the workers' premature retirement and exposure to safety  
51 and health issues (e.g., computer-vision technologies, building information modeling, wearable  
52 sensing technologies, and data mining and management) [6-10]. Moreover, these technology-  
53 based solutions help monitor and improve workers' performance by providing feedback [11-13].

54 Among these technology-based solutions, wearable sensing technologies have increased attention  
55 in recent years since they provide a wide range of opportunities for researchers and practitioners  
56 to develop automated and real-time systems for workers' safety and performance monitoring [13],  
57 in which the fundamental requirement for the workers' performance and safety assessment is  
58 activity recognition [14-17].

59 Previous studies proposed various activity recognition systems using kinematic-based  
60 methods [13,18-20], vision-based methods [11,12,21-23], and audio-based methods [15] to  
61 recognize construction worker activities. Each of these methods has its advantages and  
62 disadvantages. Computer-vision-based methods use an image or video data captured using optical  
63 cameras to provide information on worker activities. Even though vision-based methods provide  
64 semi-real-time information and reliable documentation for the future, these methods are sensitive  
65 to environmental factors, affected by obstacles, require large data storage, and high equipment cost  
66 [13]. Whereas the audio-based methods use sounds captured using audio sensors to recognize  
67 activities, they are not suitable for noisy environments and predict activities with accuracy  
68 compared to other methods [13]. Among the three methods, the kinematic-based methods have  
69 gained increased attention due to ease of use, low-cost, non-intrusive, reliable, and high accuracy  
70 activity recognition models compared to vision-based or audio-based methods [13,16,18]. The  
71 kinematic-based methods involve wearable sensors such as an inertial measurement unit (IMU)  
72 attached to the workers' body to recognize the activities' kinematic patterns. The previously  
73 proposed kinematic-based construction workers' activity recognition systems have used a  
74 smartphone or IMU sensor attached to the waist, arm, thigh, chest, and wrist to acquire  
75 accelerometer and gyroscope data of the worker performing activities such as bricklaying,  
76 carpentry, hammering, sawing, wrenching, hauling, unloading, and drilling [13,16,18,24-32].

77 Although most of the previous studies have achieved good accuracies, there are some the  
78 limitations such as restrictions on using smartphones on construction sites pose challenges for  
79 practical implementation, use of multi smartphones or IMU sensors is challenging while  
80 performing construction activities due to the dynamic nature of the construction work, and the  
81 current models have predicted few activities involving limited motions and body parts. Moreover,  
82 the recent state-of-the-art review articles on construction worker activity recognition methods [13]  
83 and wearable sensor applications in construction safety and health [6] stated that using sensor  
84 fusion and hybrid model could be the solution to obtain more precise and generalized methods to  
85 commercialize the workers' activity recognition and other construction safety applications such as  
86 fatigue monitoring or workload evaluation. Therefore, to overcome the challenges of the current  
87 construction workers' wearable sensor-based activity recognition methods, this study proposes  
88 developing automated construction workers' activity recognition using forearm electromyography  
89 (EMG) and IMU data. Moreover, this study validates the feasibility through a case study of  
90 scaffold builders who are important craft to the industrial and commercial construction projects.  
91 In the case study, forearm physiological data collected from EMG sensor and kinematic data  
92 collected from IMU sensor were analyzed for recognizing complex scaffold builder activities that  
93 involve different body parts (wrist, forearm, upper body, lower body, and whole-body) and various  
94 motions (repetitive motion, impulsive motion, and free motion) performed in a short time. To  
95 achieve the proposed objective, we first collected forearm EMG and IMU data from six  
96 participants using the armband sensor while performing scaffold builder activities from six  
97 participants. The dataset consists of 38 variables (accelerometer - 3, gyroscope – 3, and EMG –  
98 32) with approximately 150,000 datapoints. Secondly, the collected data were preprocessed and  
99 prepared for Artificial Neural Network (ANN) model building and training. Then, the ANN model

100 was trained and evaluated. Finally, the performance of the proposed model was evaluated on real-  
101 time un-labeled data and compared the performance of different sensor combinations and  
102 classification algorithm.

103 The rest of the paper is divided as follows. First, we reviewed the background and related  
104 work regarding construction workers' activity recognition using wearable sensors. Next, the  
105 proposed automatic construction workers' activity recognition model was introduced and followed  
106 by the experiment section, including model validation and performance evaluation of the proposed  
107 method. In the end, it concludes with the discussions of the findings, limitations of the study, and  
108 future research directions.

109

## 110 **2. Literature Review**

### 111 ***2.1. Human Activity Recognition, Deep Learning, and Sensor Modality***

112 An activity is defined as a group of actions that include a series of consecutive movements  
113 [13]. Human activity recognition (HAR) involves predicting a person's movement based on sensor  
114 data and machine learning models [33]. HAR is broadly classified into two types, i.e., sensor-based  
115 and vision-based [34]. The vision-based activity recognition system detects human motion using  
116 images or videos, whereas sensor-based systems focus on the motion data from smart sensors such  
117 as accelerometers, gyroscopes, electromyography, audio sensors, vibration sensors, etc. [35].

118 The wearable sensor-based activity recognition using traditional pattern recognition (PR)  
119 methods mainly involves three steps, i.e., sensor data collection, feature extraction, and model  
120 training [36]. Firstly, acquiring the data from sensors such as accelerometers, gyroscope,  
121 magnetometers, electromyography sensors, audio sensors, vibration sensors, etc. Secondly,  
122 features such as time-domain, frequency-domain, or statistical features are manually extracted

123 from the data based on human experience or domain knowledge. Finally, features are used to train  
124 the models to recognize activities [37]. The deep learning models are preferred over traditional  
125 pattern recognition (PR) because of the following reasons [35,38]:

- 126 • In traditional PR methods, the features are extracted through a heuristic and hand-crafted  
127 approach, which relies heavily on human experience and domain knowledge [39].
- 128 • From the human experience, only statistical features such as mean, median, amplitude,  
129 frequency, minimum, maximum, etc., can be learned by the models. These statistical  
130 features alone are not sufficient to recognize complex activities.
- 131 • The traditional pattern recognition methods require a large amount of labeled data for  
132 training models, whereas deep learning networks can utilize the unlabeled data for model  
133 training.
- 134 • The traditional pattern recognition models focus on training from static data, whereas in  
135 real life, the activity data is streamed real-time, which requires robust and incremental  
136 learning.

137 The deep learning models are used to overcome the limitations of traditional pattern  
138 recognition models. Unlike traditional pattern recognition models, the feature extraction and model  
139 training are performed simultaneously in the deep learning models by extracting the high-level  
140 features in deep layers, which helps recognize complex activities. In the case of extensive  
141 unlabeled data, deep generative models can exploit unlabeled data for model training. Moreover,  
142 the models trained on extensive labeled data can be transferred to new activities with few or none  
143 labels [34,35,38].

144 The sensor modalities for human activity recognition (HAR) can be classified into body-  
145 worn sensors, object sensors, ambient sensors, and hybrid sensors [38]. The body-worn sensors,

146 such as accelerometers, gyroscope, magnetometers, etc., wore on the body are among the most  
147 common modalities in HAR. The body-worn sensors are found in wristwatches, smartphones,  
148 glasses, bands, and helmets [33,35,38]. The object-worn sensors are attached to the objects to  
149 recognize the object's movement to infer human actions. The most common object-worn sensors  
150 used for HAR are radio frequency identifiers (RFID) tags and accelerometers. However, object-  
151 worn sensors are less popular than body-worn sensors due to their deployment [40].

152 In contrast, ambient sensors such as sound, radar, temperature, and pressure sensors capture  
153 the interaction between humans and the environment. Human activities are inferred based on the  
154 changes in the environment. Similar to the object-worn sensor, the ambient sensors are difficult to  
155 deploy. Moreover, only certain types of activities can be inferred using ambient sensors. In recent  
156 years, hybrid sensors (a combination of body-worn, object-worn, and ambient) is gaining  
157 importance due to the rich information of human activities provided by the sensors and improving  
158 HAR accuracy. The hybrid sensors can recognize the complex activities of multiple occupants of  
159 smart homes [41,42]. Various deep learning models such as a deep neural network (DNN),  
160 convolution neural network (CNN), recurrent neural network (RNN), deep belief network (DBN),  
161 stacked autoencoder (SAE), and hybrid models are available for HAR [35,38]. All these deep  
162 learning models are the classes of ANN which are used based on the data type. For example, CNN  
163 and RNN models are used for image/video and sequence data, respectively [43].

164 ***2.2. Wearable Sensing Technology Applications in Construction***

165 In recent years, wearable sensors are widely used in the construction industry for different  
166 applications, especially in construction safety and health. The different types of sensors widely  
167 used for construction applications are kinematic sensors (such as IMU), cardiac activity (such as  
168 Electrocardiogram (ECG or EKG), and photoplethysmogram (PPG)), skin response (such as

169 Electrodermal Activity (EDA) and Skin Temperature (ST)), eye movement (such as eye-tracking),  
170 muscle engagement (such as EMG), and brain activity (such as electroencephalogram (EEG)).  
171 IMU sensors are widely used as wearable sensors in the construction industry to measure the  
172 objects' kinematic movement, including construction workers, equipment, and tools. IMU sensors  
173 attached to workers' bodies were used to determine workers' body posture, acceleration, and  
174 orientation [44-46], and were also used for preventing musculoskeletal disorder by detecting  
175 awkward postures [47-49] and fall protection by identifying a sudden change in body acceleration  
176 [50-52]. The measure of cardiac activity using ECG and PPG sensors facilitates in determining the  
177 workers' physiological status. The metrics such as heart rate variability (HRV), inter-beat-intervals  
178 (IBI), pulse-rate variability (PRV), and heart-rate reserve (HRR) derived from heart rate are  
179 essential to determine the physical and mental condition of the workers [53,54]. The EMG sensors  
180 capture muscle activity used to assess the muscle load and forces used for ergonomic assessment  
181 [55]. The PPG, EDA, ST, and heart rate sensors were extensively used for assessing the workers'  
182 physical workload and fatigue [8,56-58]. The use of eye-tracking to measure eye positions and  
183 movements relative to the participant's head helps evaluate the construction safety training and  
184 hazard recognition abilities [59,60]. The EEG sensors which measure brain activity are used to  
185 assess the workers' mental status on the job site and the effectiveness of training programs [61,62].  
186 Even though several have shown the feasibility of using wearable sensors for construction safety  
187 and health, there exist some challenges such as noise and artifacts in field measurements,  
188 variability in standard to assess personal safety and health risks, the uncertainty of return of  
189 investments, and user resistance for adoption [6].

190

191

192 **2.3. Construction Activity Recognition**

193 Construction activity recognition helps in safety, productivity, and quality control analysis.  
194 Advancements in automated data acquisition systems to quantity progress and track resources to  
195 streamline the crew activity analysis have shown promising results compared to conventional  
196 methods such as direct observation or survey-based methods, which are time-consuming, tedious,  
197 and error-prone. However, automated data collection technologies are still being investigated for  
198 their feasibility and reliability in construction domain applications. The automated data acquisition  
199 systems can be broadly classified into vision-based and wireless sensor-based systems. The vision-  
200 based techniques have been proposed and evaluated by various researchers for activity recognition  
201 and process monitoring [63]. On the other hand, wireless sensor-based systems are assessed to  
202 collect Spatio-temporal activity data [64]. However, vision-based techniques are often prone to  
203 illumination variability and occlusions on the job site, whereas wireless sensor-based methods  
204 overcome the challenges of the line of sight (LOS) and occlusions. Moreover, sensor-based  
205 methods are a low-cost solution for activity analysis.

206 Wearable sensor-based activity recognition aims at identifying the physical actions from a set  
207 of sensor signal data, which can be achieved by utilizing machine learning techniques. The inertial  
208 measurement units (IMUs), which include accelerometer, gyroscope, and magnetometer, are the  
209 most commonly used wearables sensors used for construction activity recognition. The overall  
210 process of developing an activity recognition system using sensor signal data and machine learning  
211 techniques is as follows: raw signal data acquisition and annotation, segmentation of labeled data  
212 for feature extraction, training machine learning-based classifier algorithms, and validation of the  
213 models. Even though the framework for activity recognition using wearable sensors and ML  
214 algorithms remains the same, it is essential to investigate the feasibility of using different wearable

215 sensors for an activity or action recognition in the construction domain to improve accuracy,  
216 reliability, and usability. The model accuracy depends on various factors such as type of sensor  
217 data (acceleration, gyroscope, EMG, etc.), feature set (time-, frequency-, and discrete  
218 representation domain), classifier algorithms (k-nearest neighbor, neural network, support vector  
219 machine, and decision tree). Various studies have developed using different ML models and  
220 investigated the influence of several factors for construction activity recognition using different  
221 wearables sensors. Joshua and Varghese [65] investigated the use of wired accelerometers attached  
222 to the waist of the mason to recognize brick laying actions for productivity analysis. The study  
223 reported that the multilayer perceptron and neural network classifier algorithm best performance  
224 with 80% accuracy using features such as mean, maximum, variance, correlation, and energy.  
225 Joshua and Varghese [66] developed the accelerometer-based method for ironwork and carpentry  
226 activities classification using a decision tree with 90.07 and 77.74 percent accuracy. Cezar [24]  
227 has developed a construction activity recognition model using a dominant hand accelerometer and  
228 gyroscope data to recognize hammering, sawing, sweeping, and drilling activities with the highest  
229 accuracy of 91% Quadratic Discriminant Analysis (QDA). Khan and Sohail [25] have evaluated  
230 17 classification algorithms and three sensor positions to recognize nine construction activities.  
231 The study concluded that the waist position had achieved the highest accuracy of 93.90% for the  
232 Random Forest classifier. Moreover, Joshua and Varghese [26] have proposed a framework to  
233 select the accelerometer sensor's position to obtain the best classification results. A bricklaying  
234 case study proved that the sensor's position has a significant effect on classification accuracy.  
235 Yang, et al. [27] have developed automated near miss fall incidents in ironworkers using IMU data  
236 from waist and support vector machine (SVM), which obtained an accuracy of 91.1%. In contrast,  
237 the near-miss classification model of Lim, et al. [28] obtained an accuracy of 94% by using

238 accelerometer data from a smartphone placed at the hip pocket. Akhavian and Behzadan [29]  
239 developed a construction activity recognition and classification system using raw accelerometer  
240 and gyroscope data from a smartphone placed on the upper arm while performing sawing,  
241 hammering, wrenching, loading, hauling, and unloading. The study evaluated the performance of  
242 the classification algorithms such as K-nearest neighbor (KNN), ANN, logistic regression (LR),  
243 decision trees (DT), and support vector machine (SVM) using the features such as average,  
244 minimum, maximum, interquartile range (IQR), and root means square (RMS). The 10-fold cross-  
245 validation of the classifiers reported that the NN algorithm performed better than other classifiers  
246 with an average accuracy of 93.63%. Further, the study was extended to determine the activity  
247 duration using an ANN model with 90.74% accuracy [20]. Ryu, et al. [67] tested the feasibility of  
248 using an accelerometer-embedded wrist-worn for construction workers' action recognition such as  
249 spreading motor, laying blocks, adjusting blocks, and removing mortar precision performing  
250 bricklaying activity. The study investigated the classification accuracy of KNN, DT, multilayer  
251 perceptron, and SVM for different window sizes and features (time- and frequency -domain); the  
252 10-fold cross-validation results reported that SVM with 4s window size showed the highest  
253 classification accuracy of 88.1%. Cheng, et al. [68] developed a task-level activity analysis using  
254 the data fusion of Spatio-temporal and workers' posture data for productivity analysis. The  
255 accelerometer and gyroscope data were used to evaluate the construction workers' workload [19]  
256 and ergonomic risk [69] using an SVM classifier accuracy of 95.67% 92.7%, respectively.

257 Previous studies have proved that the sensor placement on the body significantly affects the  
258 activity recognition performance because the sensor signal pattern for the same activity varies  
259 depending on the sensor's position [70]. For activity recognition using accelerometers, the sensor's  
260 location close to the waist represents the significant body motions [71]. However, waist-oriented

261 acceleration signals do not reflect hand and arm movement, challenging to differentiate actions,  
262 including the movements [72]. The studies [73,74] reported using a single accelerometer sensor  
263 on the dominant wrist to classify daily living activities with an accuracy of around 95%. Although  
264 these studies have proved that using a single accelerometer sensor on the upper body was sufficient  
265 for recognizing construction activities, the models' robustness needs to be improved to predict real-  
266 time un-labeled data. There remains a gap in the area of construction workers' activity recognition  
267 and wearable sensors applications in the construction domain, such as sensor data fusion at various  
268 levels, robust and reliable model to recognize multiple complex construction activities, and  
269 generalization of activity recognition models to convert to the commercialized application [6,13].

270 ***2.4. Point of Departure***

271 In the construction domain, the worker activity recognition models are broadly classified into  
272 kinematic-based, vision-based, and audio-based methods. The latter two methods have technical  
273 and practical implementation challenges such as high initial cost, influence environmental factors,  
274 low accuracy, high computation cost, large storage size, and privacy concerns [13]. Whereas the  
275 kinematic-based approaches have gained increased attention for worker activity recognition due  
276 to ease of use, low cost, non-intrusive, suitable for any environment and trade, and high accuracy.  
277 Most previous studies have used smartphones as a cost-effective data collection system for  
278 recognizing workers' motion using acceleration and gyroscope signal data acquired from  
279 embedded sensors in the smartphone [49,75-78]. However, the use of smartphones for activity  
280 recognition has challenges for practical implementation. To overcome the challenges of  
281 smartphone sensors, other studies have proposed using accelerometer and gyroscope data to  
282 develop machine learning-based activity recognition models for various applications such as the  
283 activity analysis of workers, fall risk detection, ergonomic assessment, and equipment detection

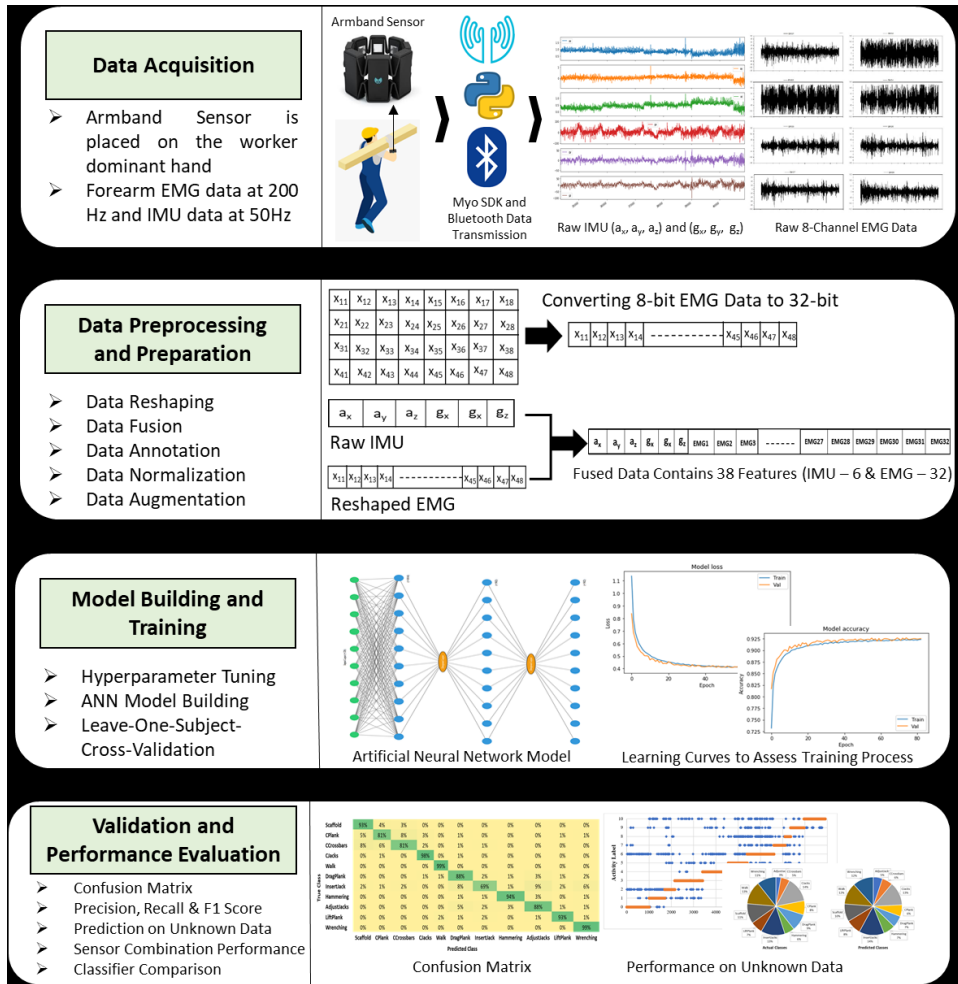
284 [18,27,41,50,79,80]. The limitations of these studies are they can identify a fewer number of  
285 construction activities involving either stationary movements or traveling (e.g., bricklaying and  
286 walking) and were limited to the forearm or upper body movements (e.g., hammering, sawing,  
287 wrenching, power drilling, and hammering) [74,81-84]. Therefore, it is essential to develop an  
288 activity recognition system to recognize complex construction activities involving different body  
289 parts (wrist, forearm, upper body, lower body, and whole-body) and various motions (repetitive  
290 motion, impulsive motion, free motion, and idle) performed in a short time interval. None of the  
291 previous studies have used other than motion data for construction worker activity recognition.  
292 Since most construction activities involve muscle activity and dynamic motion in a short interval  
293 of time, muscle activity and motion data might improve activity recognition. So, it is essential to  
294 investigate the fusion of physiological and kinematic data to improve the worker activity  
295 classification performance and recognize activities that do not involve the movement of a human  
296 body part. Other technical challenges of previous studies include the necessity of large dataset to  
297 develop models, use of multiple sensors, need for domain knowledge for feature extraction, human  
298 variability, unable to generalize the model, Moreover, there is a necessity to explore various  
299 preprocessing techniques such as data augmentation, and hyperparameter optimization to develop  
300 robust and reliable models using an optimal number of sensors.

301

### 302 **3. Research Methodology**

303 As shown in Figure 1, the proposed research methodology starts with data acquisition from a  
304 wearable armband sensor that can collect EMG and IMU data. The collected raw multi-sensor data  
305 is then preprocessed and fused to obtain a dataset with EMG and IMU data features. The fused  
306 data is labeled with the actual activity class and further used to build and train an ANN model. The

307 proposed methodology's performance is evaluated through a series of the analysis, such as the  
 308 performance on unlabeled new data, the performance of different sensor combinations, and  
 309 comparison of performance with other classification algorithms. Each of these steps is further  
 310 discussed in the following subsections.



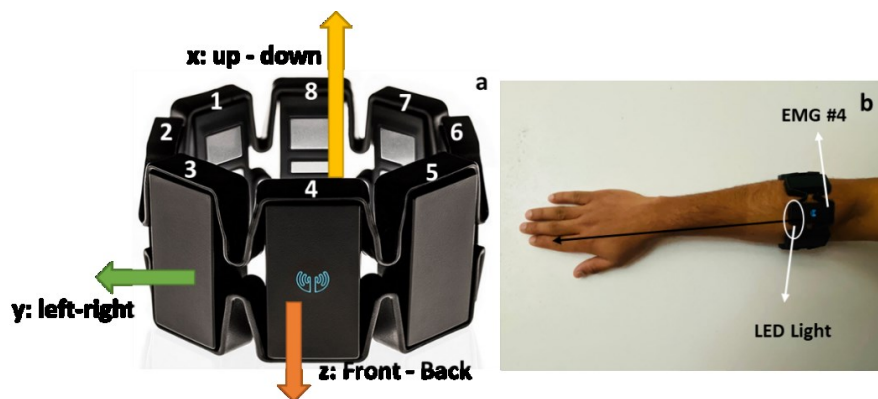
311

312 **Figure 1.** Framework for construction worker activity recognition using forearm-based EMG  
 313 and IMU armband sensor

### 314 **3.1. Data Acquisition using Forearm-based Armband Sensor**

315 A forearm-based armband sensor (Myo Armband) developed by Thalmic Labs Inc. was used  
 316 to collect forearm EMG and IMU data. This armband sensor is a non-intrusive wearable sensor  
 317 that consists of eight EMG sensors (#1-#8) and one 9-axes IMU sensor (3 for acceleration, 3 for

318 gyroscope, 3 for magnetometer, and embedded within EMG sensor #4). The armband sensor  
 319 weighs approximately 93grams and needs to be worn at the thickest part of the forearm with EMG  
 320 sensor #4 in the line of the index finger and LED light towards the lower forearm, as shown in  
 321 Figure 2. Moreover, Figure 2 shows the electrode locations and IMU axes directions. The data was  
 322 transmitted in real-time to local or cloud storage via Bluetooth Low Energy (BLE) wireless  
 323 connection. According to Thalmic Labs Inc., the Myo armband sensor has a built-in rechargeable  
 324 lithium-ion battery that can last for one full day on a single charge. The armband sensor is also  
 325 easy to use, comfortable to wear for long periods, do not obstruct ongoing work, and stable  
 326 Bluetooth connectivity. The Myo armband has achieved an acceptable system usability score  
 327 (SUS) when tested for usability in other domains such as medical [85] and entertainment [86]. The  
 328 raw EMG and IMU data can be collected from a program that we developed using the Myo  
 329 software development kit (SDK) 200 and 50 Hz. The EMG sensors capture the forearm muscle  
 330 electrical impulses, which are stored as an 8-bit array with values ranging from -128 to 127, which  
 331 is different from the data collected from conventional EMG sensor values are in a format of volts  
 332 or millivolts. In comparison, the IMU sensors capture the acceleration, angular velocity, and  
 333 orientation of the forearm along x, y, and z directions.



334

335 **Figure 2.** (a) Myo armband electrode location and IMU axes directions; (b) Myo armband  
 336 placement on the forearm

337 **3.2. Data Preprocessing and Preparation**

338 Sensor data fusion can be performed at different levels, including signal level, feature level,  
339 and decision level. The signal level data fusion involves fusing the raw sensor data, the feature  
340 level involves fusing features extracted from the sensor data, and the decision level involves fusing  
341 the decisions from outputs from sensor data [6]. In this study, the signal level sensor data fusion is  
342 considered for processing collected EMG and IMU sensor data. The signal-level fusion of the data  
343 eliminates the necessity for feature extraction from the raw data, which requires domain  
344 knowledge. Since the EMG and IMU data are collected at different frequencies, the EMG data is  
345 first reshaped to match the IMU frequency, which is performed by transposing four rows of 8-bit  
346 EMG data to 32-bit data. The reshaped 32-bit EMG data is then fused with the IMU data of each  
347 activity using concatenation. The fused data are manually annotated using the class label shown  
348 in Table 1. The manual annotation process involves assigning activity ID to each row of the dataset  
349 since the training data will be collected for each activity. Since the EMG and IMU data obtained  
350 using armband sensors are in different units, the data is normalized using the z-score  
351 standardization (feature scaling) technique. The z-score is calculated by subtracting each feature's  
352 mean from that feature's values and then dividing the corresponding value by the standard  
353 deviation of that feature, as shown in Equation 1. This transforms the data to have a mean value  
354 as zero and standard deviation as one. Feature scaling is essential for neural network models to  
355 handle data smoothly. Feature scaling is essential for a neural network to handle the data smoothly.  
356 If the input data has units in different scales, the features with high range values may get higher  
357 derivatives during backpropagation than the features with low range values. Hence, the weights in  
358 the connected layers will be updated abnormally, and there will be a bias added to the model.  
359 Standardizing makes the model update the weights effectively during forward and backward

360 propagation and avoid model weights and errors. Moreover, it helps in faster convergence of  
361 gradient descent to the global minima. After performing standardization, all features have been  
362 reduced to the same scale [87].

$$\text{Z-score} = \frac{x_i - \bar{x}}{\sigma} \quad (1)$$

363 A large amount of synthetic data can be generated using time series data augmentation  
364 techniques to improve the ANN model's performance and prevent overfitting the model  
365 parameters. Also, data augmentation helps in the model's generalization since it introduces  
366 variability in the data without altering the labels. To account for those factors, various  
367 augmentation techniques are available such as time-wrapping, pooling, drifting, and reversing.  
368 Time-warping has a spatial-temporal characteristic that can generate data with a different warping  
369 ratio for different activities and is controlled by a number of speed changes and the maximal ratio  
370 of max/min speed. Pooling makes the data reduce the temporal resolution without a change in  
371 length. In contrast, the drift changes the data randomly and smoothly and is controlled by  
372 parameters like several drift points and maximal drift. Finally, the reverse will help in reversing  
373 the timeline in a series of data. Each augmentation technique generates a 1-fold increase in training  
374 data, resulting in a 4-fold increase in the number of data points for each user [40,70].

### 375 ***3.3. Model Building, Training, and Evaluation***

376 An ANN-based deep learning model is proposed for construction worker activity recognition.  
377 An ANN model can handle complex data by recognizing the hidden patterns in the data and sensing  
378 the linear and non-linear relationship between independent and dependent variables by reducing  
379 the noise in the data. In this study, the ANN model is built in Keras [88], a high-level neural  
380 networks application programming interface (API), written in Python and capable of running on  
381 top of TensorFlow. The model building and training module involve three essential steps, i.e.,

382 hyperparameter optimization, model building and compiling, and model training. Each of these  
383 steps is discussed in this section.

384 *3.3.1. Hyperparameter Optimization*

385 ANN network is designed with significant hyperparameters to achieve desirable activity  
386 classification results. To obtain the best classification results, one needs to tune the model with  
387 different combinations of hyperparameters, where the manual tuning process is time-consuming  
388 and inefficient. To overcome the manual tuning process challenges, various automated  
389 hyperparameter optimization techniques were proposed, such as grid search, random search, and  
390 Bayesian optimization [89]. Each of these techniques has its advantages and disadvantages. A grid  
391 search method selects the grid of parameters and tries every combination to select the best  
392 parameters. However, this method is computationally expensive and takes a long time to complete.  
393 A random search does not select all the combinations but a random list of parameters and select  
394 the best parameters among those combinations. Even though it is computationally efficient, it can  
395 probably miss some of the crucial parameters during the evaluation, which is unreliable due to its  
396 random selection. In contrast, Bayesian optimization keeps track of the past evaluated results and  
397 builds a probabilistic model to map the hyperparameters to the objective function's probability  
398 score. They perform better based on a surrogate function, which can help identify the global  
399 minima. In this study, the tree-structured Parzen Estimator (TPE) based surrogate model has been  
400 used, a sequential model-based optimization (SMBO) approach [89]. TPE is represented as  $p(y|x)$ ,  
401 where y is the quality Score, and x represents hyperparameters, as shown in Equation 2.

402 
$$p(y|x) = \frac{p(x|y) * p(y)}{p(x)} \quad (2)$$

403  $p(x|y)$  is a probability of hyperparameters given the value of an objective function, as shown in  
404 Equation 3.

405 
$$p(x|y) = \begin{cases} l(x) & \text{if } y < y^* \\ g(x) & \text{if } y \geq y^* \end{cases} \quad (3)$$

406  $l(x)$  and  $g(x)$  are two different distributions of hyperparameters with  $l(x)$  used when the  
 407 value of an objective function is less than the threshold, and  $g(x)$  is used when the objective  
 408 function's value is more significant than a threshold.  $Y^*$  is the threshold value. TPE draws a sample  
 409 of hyperparameters from  $l(x)$  and returns the parameters which yielded the highest value with the  
 410 ratio  $l(x)/g(x)$ . Overall, the algorithm selects a new set of hyperparameters, evaluates the model,  
 411 and stores them as history. With every iteration and using the history,  $l(x)$  and  $g(x)$  is built by  
 412 an algorithm to evaluate the objective function's probability model. Since the algorithm suggests  
 413 better candidate hyperparameters for evaluation, the objective function score increases much faster  
 414 than random or grid search results in less total evaluations of the objective function. Also, TPE  
 415 can reduce the running time and get the best scores on test data. Sequential model-based  
 416 optimization approaches vary like the surrogate, but all depend on the knowledge from previous  
 417 studies to suggest better hyperparameters for the next evaluation. TPE is an algorithm that uses  
 418 Bayesian reasoning to create a surrogate model and can use expected improvement to pick the next  
 419 hyperparameter.

420 *3.3.2. Model Building and Compiling*

421 In a neural network architecture, many crucial parameters need to be considered to develop an  
 422 efficient model. The most important features are the numbers of hidden layers, neurons in each  
 423 layer, optimizers, activation functions, learning rate, batch size, epochs, and regularization. The  
 424 number of layers and neurons in each layer depends on the data where the input and output layer  
 425 nodes are equal to input features and the number of activity classes, respectively. The optimizers  
 426 in neural networks change attributes such as weights and learning rate to reduce the losses. Adam  
 427 optimizer is the most commonly used algorithm, an adaptive learning technique for each weight

428 in the neural network; it uses the estimates of both first and second moments of gradient and  
429 evaluates individual learning rates for different parameters. Adam optimizer is considered an  
430 improvised version of well-known optimizers such as RMSProp, AdaGrad, and SGD [90]. It uses  
431 the functional combination of RMSProp and SGD by using squared gradients and moving average  
432 of gradients for effective faster convergence to global minima.

433 The ReLu activation function is used for input and hidden layers. Compared with other  
434 functions like sigmoid and tanh, ReLu can handle large layers and tackle the vanishing gradient  
435 issue. For the output layer, the Softmax activation function is applied since it is useful for multi-  
436 label classification. Also, Softmax best suits for output layer as it gives the probability values for  
437 predicting different classes. The choice of batch size decides the number of samples from the  
438 training data propagated through the network. Whereas the epoch decides the number of times, all  
439 the training samples are passed forward and backward through a neural network. If the class labels  
440 were mutually exclusive, the sparse categorical cross-entropy loss function should be applied to  
441 the model. Moreover, it is essential to convert target variables into integers for the ANN model.

442 Regularization involves concepts such as  $L_1$  and  $L_2$  regularization, dropout, and early  
443 stopping. Firstly,  $L_1$  and  $L_2$  are lasso and ridge regressions, which add a penalty to the loss  
444 function. The loss function is the ordinary least square technique that measures the sum of the  
445 squared errors. They are used for feature selection and removing multicollinearity during model  
446 training. Both are involved in the process of reducing the weights or coefficients of neural network  
447 function.  $L_1$  reduces the weights faster than  $L_2$  and finally makes the model more straightforward  
448 and reduces overfitting. Each has its advantages and disadvantages, but elastic net regularization  
449 has been used to optimize the model in the best possible way, combining  $L_1$  and  $L_2$  regularizations.  
450 Secondly, the dropout function reduces the number of neurons required for training in a selected

451 layer for each iteration to prevent overfitting. The dropout ratio increase eventually results in  
452 underfitting curves. Finally, early stopping is another regularization method that helps stop the  
453 model training when the validation loss is no longer decreasing or increasing after performing a  
454 certain number of epochs. Early stopping is considered one of the best solutions to tackle the  
455 overfitting problem.

456 *3.3.3. Model Training*

457 During model training, backpropagation involves the multiplication of gradients in every layer.  
458 If the gradient values are too small, the models suffer from vanishing gradient problems, but if the  
459 gradient values are too high, the model suffers from an exploding gradient problem. Selecting a  
460 set of optimized parameters plays a significant role in providing an accurate predictive model.  
461 Once the optimum parameters are selected through hyperparameter optimization, the model is  
462 diagnosed for the underfitting or overfitting issues using learning curves. The learning curves, such  
463 as model loss and accuracy, help understand the model's learning performance over time during  
464 training. Moreover, the model curves can be used to diagnose the problems of under and  
465 overfitting. Two metrics used to assess the performance of learning are loss (error) and accuracy.  
466 For a better learning performance, the model loss (error) should be decreasing, and the model  
467 accuracy should be increasing. The training learning curve measured on training data indicates  
468 how well the model is learning, whereas the validation learning curve calculated on validation  
469 data, which is not part of training data, represents how well the model is generalizing. The learning  
470 curves' shape and dynamics help diagnose the model's behavior and identify if the model has under  
471 fitted or a good fit or overfitted. The model's underfitting occurs when the model cannot learn the  
472 training dataset, whereas overfitting refers to a model that has leaned the training data too well,  
473 including random fluctuations and noise in the data. A good fit model exists between underfitting

474 and overfitting models, which can be identified from learning if the loss curve decreases to the  
475 point of stability and has a small gap between the training and validation curve. The learning curves  
476 are developed using the Keras callback history, which records the loss and accuracy of training  
477 and validation dataset for each epoch. The batch size and epochs are set to 100 and 150,  
478 respectively. To overcome overfitting or underfitting, the regularization concept has also been  
479 implemented during the model training.

480 *3.3.4. Model Evaluation Technique*

481 General evaluation of machine learning models can be done by splitting the collected  
482 experiment data into train and test data. However, the disadvantage with this technique is that the  
483 model's evaluation is done specifically on this split data where they can have data leakage between  
484 the train and test on the same subject, especially in human activity recognition and testing any new  
485 or unseen data on the trained model may not be reliable [36]. In order to avoid this and make a  
486 generalized model, the cross-validation technique has been used. Cross-validation is a technique  
487 that holds out test data from a given data in an experiment, trains the model on the remaining data,  
488 and tests it on the formerly reserved test data. This process is repeated for the K number of  
489 experiments for the entire training data. Splitting of the data depends on the number of splits we  
490 required and is represented by K, where K is the number of folds. Depending on the given input  
491 parameter K, the K number of experiments will be performed to evaluate the model performance.  
492 Popular cross-validation techniques are K-fold, Stratified K-fold, Repeated K-fold, Leave One  
493 Out, Leave One Subject Out, and Nested. The dataset consists of different construction activities  
494 performed by different subjects. So, in this study, Leave-One-Subject-Out (LOSO) cross-  
495 validation technique has been chosen. LOSO is a K-fold cross-validation technique where the  
496 number of folds is chosen before the model evaluation. In LOSO, the number of folds is equal to

497 the number of subjects who performed their activities in our experiment, and LOSO evaluates each  
498 subject's accuracy in different folds or experiments. Hence, LOSO performance is robust. The  
499 LOSO's overall accuracy is determined by finding the average of all the folds in our experiment  
500 [91].

501 ***3.4. Performance Evaluation Metrics***

502 Once a good fit model is obtained through the training and validation process, the built ANN  
503 model's performance will be evaluated by the testing dataset using classification accuracy,  
504 confusion matrix, precision, recall, and F1 Score. The most general and first look evaluation for  
505 any deep learning techniques are done by classification accuracy. It is calculated as the number of  
506 correctly predicted outcomes to the total number of predictions. Higher classification accuracy is  
507 required to achieve the desired activity recognition results. However, the classification accuracy  
508 alone is not sufficient to decide the robustness and reliability of classification results. Therefore,  
509 other metrics such as precision, recall, and F1 Score of the proposed model are also analyzed. A  
510 confusion matrix is a matrix with an equal number of rows and columns. It represents the complete  
511 performance of the model considering each class. Each row and column of the matrix corresponds  
512 to true and predicted classes. The diagonal cells of the matrix represent the percentage of correct  
513 prediction for each class, and the off-diagonal elements represent the misclassification percentage  
514 with respect to other classes. In order to understand the concept of precision and recall, firstly  
515 following terms are defined, True Positive (TP), True Negative (TN), False Positive (FP), and  
516 False Negative (FN) come into the picture. TP is the number of correct positive predictions done  
517 by a positive model. TN refers to the number of negative predictions done by a model that is  
518 negative. FP is the number of classes predicted incorrectly where the model thinks predicted  
519 classes are positive (true) but, it is not true. FN is the only misclassified metric where the model

520 thinks the predicted activity is not positive (true), but it is true. For the multi-classification model,  
 521 the values of TP, TN, FP, and FN were calculated using the confusion matrix where TP – value in  
 522 the diagonal cell, FN – for a class is the sum of values in the corresponding column excluding TP  
 523 value, and FP – for a class is the sum of values in the corresponding rows excluding TP value.  
 524 Using the TP, TN, and FN values, the metrics precision and recall were calculated using Equations  
 525 2 and 3, respectively. The prediction value indicates how often the prediction is correct, which is  
 526 defined as the ratio of the number of true positive predictions (TP) to all total number of positive  
 527 predictions of the model (TP+FP) (Equation 4). In contrast, the recall indicates the correctly  
 528 predicted rate of a class, which is the ratio of the number of true positive predictions (TP) to a total  
 529 number of predictions (TP+FP) (Equation 5).

$$\text{Precision} = \frac{\text{TP}}{\text{TP} + \text{FP}} = \frac{\text{Value of the Diagonal Cell of the Class}}{\text{Total Number of Predictions of the Class}} \quad (4)$$

$$\text{Recall} = \frac{\text{TP}}{\text{TP} + \text{FN}} = \frac{\text{Value of the Diagonal Cell of the Class}}{\text{Total Number of Instances of the Class}} \quad (5)$$

530 If the classes are imbalanced, the most useful and reliable metric to assess the model  
 531 performance is the F1 Score, a harmonic mean of precision and recall, as shown in Equation 6.

$$\text{F1 Score} = 2 * \frac{\text{Precision} * \text{Recall}}{\text{Precision} + \text{Recall}} \quad (6)$$

532 The above formulas are used to calculate the performance metrics for individual classes,  
 533 whereas the weighted precision, recall, and F1 Score following Equation 7 are applied to evaluate  
 534 the overall model performance. The weighted average of a metric is the sum of the metric  
 535 (precision, recall, and F1 Score) multiplied by the samples of each class (i), then divided by the  
 536 samples of all the classes.

$$\text{Weighted Metric} = \frac{\sum_{i=1}^m (\text{Metric}_i) * (\text{Samples}_i)}{\sum_{i=1}^m \text{Samples}_i} \quad (7)$$

537 Where  $m$  is the total number of classes,  $\text{Metric}_i$  is the value of metric for class  $i$  ( $i = 1, 2, \dots, m$ ),  
 538 and  $\text{Samples}_i$  is the number of samples in each class  $i$  ( $i = 1, 2, \dots, m$ ).

539 In addition to the performance evaluation of the proposed model, another analysis is  
 540 conducted to evaluate the activity prediction accuracy on an entirely new dataset, i.e., an unknown  
 541 dataset. We also compare the results with other classification algorithms to examine the robustness  
 542 of the proposed model. The new dataset's prediction includes performing activity recognition using  
 543 the proposed model on the dataset that is not used either in the training or testing process.  
 544 Moreover, the data was collected from an individual who performed a whole sequence of activities  
 545 at his own pace. The proposed model's performance is compared with the most common  
 546 classification algorithms previously used in other construction activity recognition studies [13].

547

#### 548 **4. System Feasibility Validation and Performance Evaluation**

##### 549 ***4.1. Case Study of Scaffold Builder Activities***

550 To validate and evaluate the proposed construction worker activity recognition model's  
 551 performance, a case study of scaffold builder activities was considered since it involves various  
 552 body parts and different movements, which allows testing the proposed model on complex  
 553 construction activities. According to OSHA, a scaffold is defined as an elevated, temporary  
 554 structure [92]. Based on the construction work, the type of scaffold may vary. Two basic types of  
 555 scaffolds are supported and suspended scaffolds. The supported scaffolds consist of one or more  
 556 platforms supported by load-bearing or rigid supports, whereas the suspended scaffold is supported  
 557 by an overhead structure using non-rigid support such as ropes [92]. The supported scaffolds are  
 558 extensively used in industrial and commercial construction projects [93]. The scaffold building

559 requires scaffold erection skills, carpentry hand tools, and heavy labor-intensive tasks [94]. By  
 560 reviewing various scaffolding activities onsite and online, we have recognized fifteen common  
 561 activities in building a supported scaffold. The activities include carrying a metal 5 ft. x 5ft.  
 562 scaffold frame (38 Lbs.) sideward, carrying a 6 ft. x 12 in. wooden plank (15 Lbs.), carrying a 7  
 563 ft. x 4 ft. scaffold cross brace (10 Lbs.), carrying 24 in. leveling jacks (6.5 Lbs.), walking around,  
 564 dragging wooden plank along the frame, lifting the plank from elbow to overhead, adjusting and  
 565 inserting the leveling jacks, hammering, wrenching, climbing stairs with and without tool bag, and  
 566 walking downstairs with and without tool bag to set up and fix scaffold pin. The fifteen scaffold  
 567 builder activities and the activity ID used for the ANN model are summarized in Table 1. Some of  
 568 the key scaffold builder activities are shown in Figure 3. All these activities require extensive  
 569 manual efforts and involve different body parts (wrist, forearm, upper body, lower body, and  
 570 whole-body) movements, and various motions (such as repetitive motion, impulsive motion, and  
 571 free motion). Moreover, it involves manual material handling tasks such as carrying different  
 572 weights, lifting at different heights, and pushing activities.

573 **Table 1.** Scaffold builder activities and activity ID

<b>ID No.</b>	<b>Activity Description</b>	<b>Activity ID</b>
0	Adjusting Leveling Jacks	AdjustJacks
1	Carrying Crossbars	CCrossbars
2	Carrying Leveling Jacks	CJacks
3	Carrying Scaffold Plank	CPlank
4	Carrying Scaffold Frame	CScaffold
5	Dragging Scaffold Plank	DragPlank
6	Hammering	Hammering
7	Inserting Jacks into Scaffold Frame	InsertJack
8	Lifting Scaffold Plank from Elbow to Overhead	LiftPlank
9	Walking	Walk
10	Wrenching	Wrenching
11	Climb	Climb
12	Downstairs	Downstairs
13	Climb with Tool Bag	ClimbW
14	Downstairs with Tool Bag	GDownstairsW



574

575 **Figure 3.** Shows few scaffold builder activities performed in outdoor environment (a) scaffold  
 576 carrying, (b) plank carrying, (c) crossbars carrying, (d) leveling jacks carrying, (e) adjusting  
 577 leveling jacks, and (f) insert leveling jacks into the scaffold

578 **4.2. Experiment Setup**

579 **4.2.1. Data Collection and Augmentation**

580 To validate the feasibility and evaluate the proposed automated activity recognition model's  
 581 performance using forearm EMG and IMU data, an experiment was performed, which involved  
 582 participants performing scaffold builder activities in the outdoor environment. Seven male college  
 583 students have voluntarily participated in the experiment. The participants' age ranged from 24 to  
 584 28 years (mean  $\pm$  SD:  $26.43 \pm 1.40$  years), weight ranged from 62.60 to 100 kgs (mean  $\pm$  SD: 80.98  
 585  $\pm$  13.38 kg), and height ranged from 1.65 to 1.83 m (mean  $\pm$  SD:  $1.73 \pm 0.06$  m). All participants  
 586 are right-handed, healthy, and have no musculoskeletal disorders record. None of the participants  
 587 have prior scaffold building experience, but all the activities were demonstrated to all the  
 588 participants before starting the experiment. The armband sensor was placed on the dominant hand

589 of each participant during the experiment. Each activity was clearly explained to the participants  
590 and asked to perform the activity for at least 30 seconds, with enough rest provided between the  
591 activities. EMG and IMU data collected from the participants' forearms were transmitted to the  
592 computer via Bluetooth, and the data were stored and labeled with the activity ID. The six  
593 participants' data were used for model building and evaluation, whereas the seventh participant  
594 (age = 26 years, weight = 76 kgs., and height = 1.65 m) was asked to perform all the activities in  
595 any sequence without any time constraint. The seventh participant's data (referred to as the new  
596 unlabeled data previously) was used to test the performance of the proposed ANN model. The  
597 whole experiment of the seventh participant was videotaped and later used for evaluating the model  
598 performance. The six participants' dataset was manually labeled, and it consists of 38 features  
599 (EMG – 32, Acc -3, and Gyro – 3) with 149,491 samples. Therefore, the input layer's size was  
600 defined as 38 nodes or neurons to hold the 38 raw data features, whereas the number of nodes in  
601 the output layer is equal to a number of activities (i.e., 15). Moreover, each activity's sample count  
602 is different since the participants performed each activity for a different duration. The imbalanced  
603 classes represent a real scenario because not all construction activities are performed for the same  
604 duration.

605 Once the field data was collected and labeled, data augmentation techniques such as time-  
606 wrapping, pooling, drifting, and reversing were applied to each user data, which increases the data  
607 by 4-folds. The number of samples per participant before and after the data augmentation are  
608 22,000 and 88,000, respectively. Therefore, the total number of samples for all the participants  
609 after the data augmentation is 524,218.

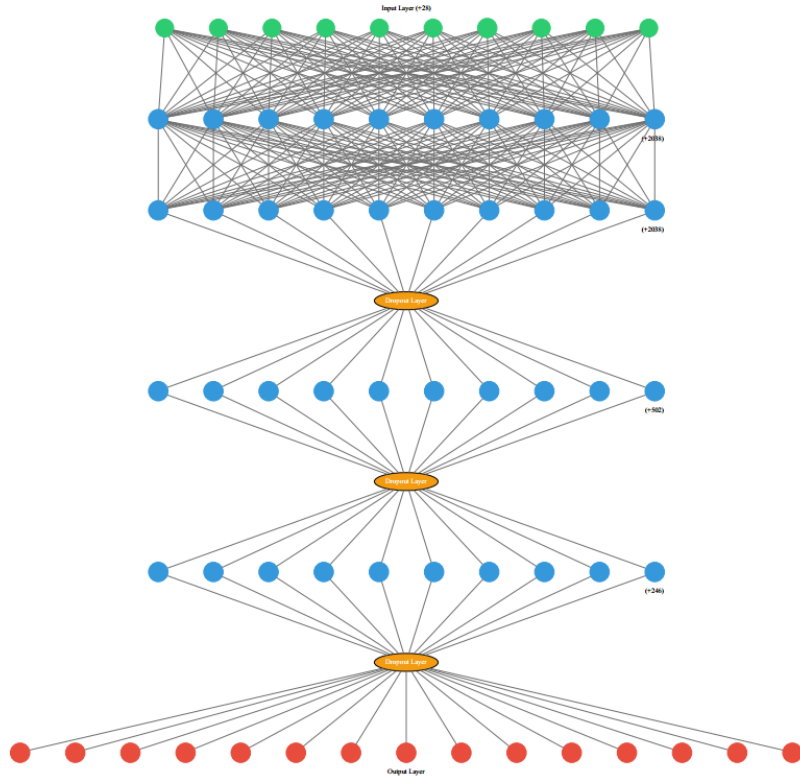
610 *4.2.2. Hyperparameter Optimization and ANN Model*

611 The optimum hyperparameters were determined using the Bayesian TPE algorithm are set  
612 to a wide range to test different combinations, as shown in Table X. From the Bayesian TPE results,  
613 it can be observed that optimum performance was achieved for the ANN architecture shown in  
614 Figure 4. The parameters for the optimized model include four hidden layers, two dropout layers,  
615 no. of neurons for hidden layers as [2048, 2048, 512, 256], batch size = 256, epochs = 100,  
616 optimizer = Adam, and activation function = ReLu. Since the batch size of 256 is used during the  
617 model training, 256 samples from training data will be used and sent to the network in both forward  
618 and backward propagation. The number of epochs selected for model training is 100, which means  
619 the model will train 100 times for the selected batches. Since the proposed model uses the early  
620 stopping function, it stops the model training process once the model performance is stable. To  
621 overcome overfitting or underfitting, the regularization concept has also been implemented during  
622 the model training.

623 **Table X.** Parameters used for Bayesian Tree-structure Parzen Estimator optimization

Parameter	#	Values
No. of Hidden Layers	7	1 to 7
No. of Neurons	6	64, 128, 256, 512, 1024, 2048
No. of Dropout Layers	5	0.1, 0.2, 0.3, 0.4
Batch Sizes	3	128, 192, 256
Epochs	3	50, 100, 150
Optimizers	3	SGD, Adam, RMSprop
Activation Functions	3	ReLu, Tanh, Sigmoid

624



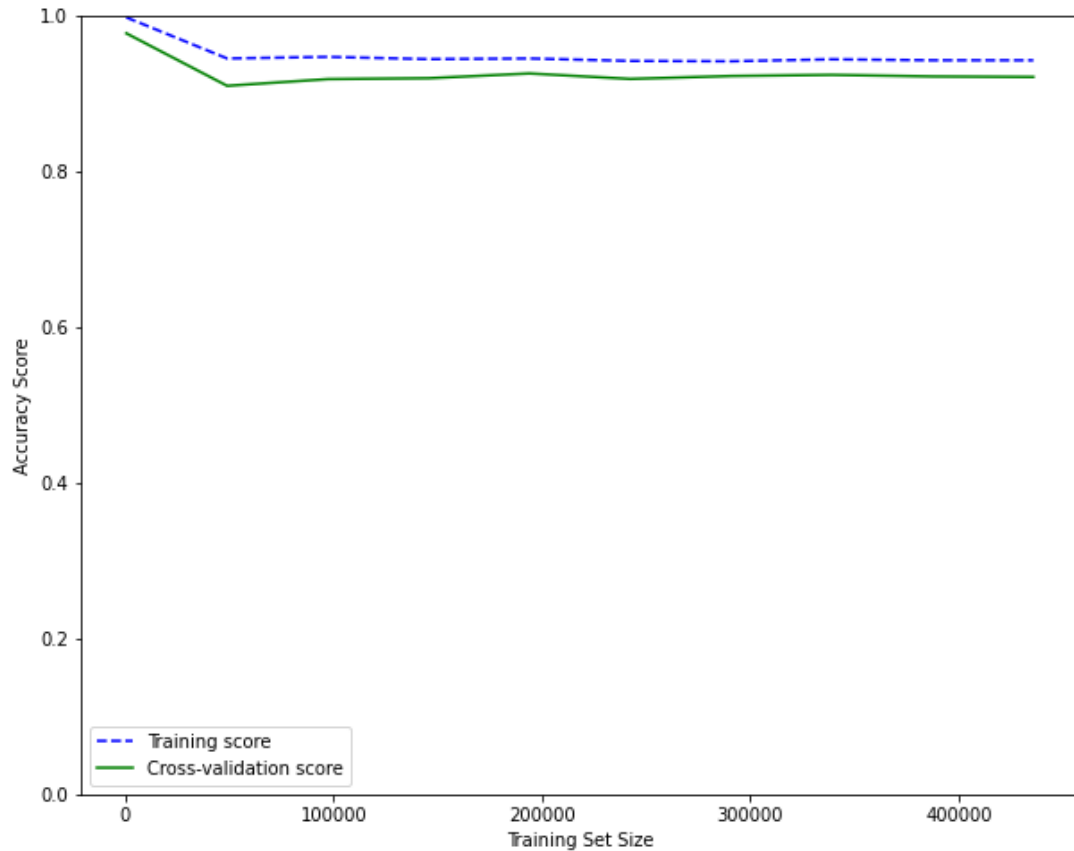
625

626 **Figure 4.** Optimal artificial neural network architecture for scaffold builder activities  
 627 prediction

628 **4.3. Model Learning Curves**

629 To assess the model performance and achieve the bias-variance trade-off, learning curves have  
 630 been plotted. Learning curves show the relation between training instances and accuracy. These  
 631 curves show the plot of training and cross-validation scores from a given model with different  
 632 training sizes and using these curves can help understand how the training and cross-validation  
 633 scores are moving as the number of training instances increase. These curves tell whether the  
 634 model is suffering from bias or variance. Leave One Subject Out (LOSO) cross-validation has  
 635 been used to generate these learning curves. Figure 5 shows the plots of training and cross-  
 636 validation scores between accuracy and different training set sizes. Ten different training set sizes  
 637 have been used. The model slightly shows underfitting for the initial training set, but as the training

638 size increases, the curves are so close and stable with low bias and low variance. Moreover, the  
639 graph shows the increase in model generalization with an increase in the training set. Average  
640 training and cross-validation scores generated from the learning curves are 94.90% and 93.29%.



641

642 **Figure 5.** Learning curve of the proposed ANN model using EMG and IMU data

643 **4.4. Performance Evaluation on Testing Data**

644 After training the model, performance evaluation is required to understand the model's  
645 overall and class performance. Leave One Subject Out (LOSO) Cross-validation has been  
646 performed, and it splits the data into train and test based on the number of subjects. In each  
647 experiment or fold, one of the subjects is used as test data, and the remaining subjects are used as  
648 training data. As our data has six users, six experiments are performed by LOSO to evaluate the  
649 model performance using confusion matrix and classification report. Figure 6 shows the

650 normalized confusion matrix of the proposed ANN model generated after cross-validation on the  
651 six subjects where X and Y axes represent the predicted and true classes. The diagonal cells  
652 represent the percent of correctly classified instances, whereas the off-diagonal elements represent  
653 the percent of misclassified instances for each activity. From Figure 6, it can be observed that the  
654 "Downstairs" (0.13) activity was highly misclassified among all other classes, followed by  
655 "AdjustJacks" with values (0.03), "Climb" (0.03), and "GDownstairsW" (0.03). The highest  
656 misclassification of "Downstairs" was identified with "Walk." Whereas, the highest classification  
657 was observed in "Hammering" (0.99), "CJacks" (0.97), "CScaffold" (0.97) and "ClimbW" (0.97)  
658 followed by "LiftPlank" (0.96), and " GDownstairsW " (0.96). Table 2 presents the precision,  
659 recall, and F1 score values for all the activities. The "Hammering" (0.99), "CJacks" (0.97), and  
660 "ClimbW" (0.97) activities shows highest precision. Whereas the least precision value of 0.86 was  
661 observed in "Downstairs." The highest recall value of 0.98 was observed in "CJacks" followed by  
662 "Wrenching" (0.97), "GDownstairsW" (0.97), and "LiftPlank" (0.97), whereas the lowest recall  
663 value was observed in "Downstairs" (0.89). Similarly, the F1 score is highest for "Hammering"  
664 (0.97), "CJacks" (0.97), and " LiftPlank " (0.97) and lowest is for "Downstairs" (0.87). The overall  
665 prediction accuracy of 93.68% was obtained on the testing dataset with 0.94 weighted average  
666 precision, recall, and F1 Score.

True Labels	AdjustJacks	0.91	0.00	0.00	0.00	0.02	0.02	0.03	0.01	0.00	0.00	0.00	0.00	0.00	0.00	0.00
	CCrossbars	0.00	0.94	0.00	0.02	0.01	0.00	0.00	0.00	0.00	0.00	0.00	0.00	0.00	0.01	0.00
	CJacks	0.00	0.00	0.97	0.01	0.00	0.00	0.00	0.00	0.00	0.00	0.00	0.00	0.00	0.01	0.01
	CPlank	0.00	0.02	0.00	0.95	0.01	0.00	0.00	0.00	0.00	0.00	0.00	0.00	0.00	0.01	0.00
	CScaffold	0.00	0.01	0.00	0.01	0.97	0.00	0.00	0.00	0.00	0.00	0.00	0.00	0.00	0.01	0.01
	DragPlank	0.01	0.00	0.00	0.01	0.00	0.93	0.00	0.02	0.01	0.00	0.00	0.00	0.00	0.01	0.00
	Hammering	0.01	0.00	0.00	0.00	0.00	0.99	0.00	0.00	0.00	0.00	0.00	0.00	0.00	0.00	0.00
	InsertJack	0.01	0.01	0.00	0.00	0.01	0.01	0.00	0.94	0.01	0.00	0.01	0.00	0.00	0.00	0.00
	LiftPlank	0.00	0.00	0.00	0.00	0.00	0.00	0.01	0.96	0.01	0.00	0.00	0.00	0.01	0.00	0.00
	Walk	0.00	0.00	0.00	0.00	0.00	0.00	0.00	0.00	0.87	0.00	0.03	0.10	0.00	0.00	0.00
	Wrenching	0.02	0.00	0.00	0.00	0.00	0.00	0.02	0.01	0.00	0.00	0.95	0.00	0.00	0.00	0.00
	Climb	0.00	0.00	0.00	0.00	0.00	0.00	0.00	0.00	0.03	0.00	0.96	0.01	0.00	0.00	0.00
	Downstairs	0.00	0.00	0.00	0.00	0.00	0.00	0.00	0.00	0.13	0.00	0.01	0.86	0.00	0.00	0.00
	ClimbW	0.00	0.00	0.01	0.01	0.00	0.00	0.00	0.00	0.00	0.00	0.00	0.00	0.00	0.97	0.01
	GDownstairsW	0.00	0.00	0.00	0.00	0.01	0.00	0.00	0.00	0.00	0.00	0.00	0.00	0.03	0.96	0.96
	AdjustJacks	0.91	0.00	0.00	0.00	0.00	0.02	0.02	0.03	0.01	0.00	0.00	0.00	0.00	0.00	0.00
	CCrossbars	0.00	0.94	0.00	0.02	0.01	0.00	0.00	0.00	0.00	0.00	0.00	0.00	0.00	0.01	0.00
	CJacks	0.00	0.00	0.97	0.01	0.00	0.00	0.00	0.00	0.00	0.00	0.00	0.00	0.00	0.01	0.01
	CPlank	0.00	0.02	0.00	0.95	0.01	0.00	0.00	0.00	0.00	0.00	0.00	0.00	0.00	0.01	0.00
	CScaffold	0.00	0.01	0.00	0.01	0.97	0.00	0.00	0.00	0.00	0.00	0.00	0.00	0.00	0.01	0.01
	DragPlank	0.01	0.00	0.00	0.01	0.00	0.93	0.00	0.02	0.01	0.00	0.00	0.00	0.00	0.01	0.00
	Hammering	0.01	0.00	0.00	0.00	0.00	0.99	0.00	0.00	0.00	0.00	0.00	0.00	0.00	0.00	0.00
	InsertJack	0.01	0.01	0.00	0.01	0.01	0.00	0.00	0.94	0.01	0.00	0.01	0.00	0.00	0.00	0.00
	LiftPlank	0.00	0.00	0.00	0.00	0.00	0.00	0.01	0.96	0.01	0.00	0.00	0.00	0.01	0.00	0.00
	Walk	0.00	0.00	0.00	0.00	0.00	0.00	0.00	0.00	0.87	0.00	0.03	0.10	0.00	0.00	0.00
	Wrenching	0.02	0.00	0.00	0.00	0.00	0.00	0.02	0.01	0.00	0.00	0.95	0.00	0.00	0.00	0.00
	Climb	0.00	0.00	0.00	0.00	0.00	0.00	0.00	0.00	0.03	0.00	0.96	0.01	0.00	0.00	0.00
	Downstairs	0.00	0.00	0.00	0.00	0.00	0.00	0.00	0.00	0.13	0.00	0.01	0.86	0.00	0.00	0.00
	ClimbW	0.00	0.00	0.01	0.01	0.00	0.00	0.00	0.00	0.00	0.00	0.00	0.00	0.00	0.97	0.01
	GDownstairsW	0.00	0.00	0.00	0.00	0.01	0.00	0.00	0.00	0.00	0.00	0.00	0.00	0.03	0.96	0.96
	AdjustJacks	0.91	0.00	0.00	0.00	0.00	0.02	0.02	0.03	0.01	0.00	0.00	0.00	0.00	0.00	0.00
	CCrossbars	0.00	0.94	0.00	0.02	0.01	0.00	0.00	0.00	0.00	0.00	0.00	0.00	0.00	0.01	0.00
	CJacks	0.00	0.00	0.97	0.01	0.00	0.00	0.00	0.00	0.00	0.00	0.00	0.00	0.00	0.01	0.01
	CPlank	0.00	0.02	0.00	0.95	0.01	0.00	0.00	0.00	0.00	0.00	0.00	0.00	0.00	0.01	0.00
	CScaffold	0.00	0.01	0.00	0.01	0.97	0.00	0.00	0.00	0.00	0.00	0.00	0.00	0.00	0.01	0.01
	DragPlank	0.01	0.00	0.00	0.01	0.00	0.93	0.00	0.02	0.01	0.00	0.00	0.00	0.00	0.01	0.00
	Hammering	0.01	0.00	0.00	0.00	0.00	0.99	0.00	0.00	0.00	0.00	0.00	0.00	0.00	0.00	0.00
	InsertJack	0.01	0.01	0.00	0.01	0.01	0.00	0.00	0.94	0.01	0.00	0.01	0.00	0.00	0.00	0.00
	LiftPlank	0.00	0.00	0.00	0.00	0.00	0.00	0.01	0.96	0.01	0.00	0.00	0.00	0.01	0.00	0.00
	Walk	0.00	0.00	0.00	0.00	0.00	0.00	0.00	0.00	0.87	0.00	0.03	0.10	0.00	0.00	0.00
	Wrenching	0.02	0.00	0.00	0.00	0.00	0.00	0.02	0.01	0.00	0.00	0.95	0.00	0.00	0.00	0.00
	Climb	0.00	0.00	0.00	0.00	0.00	0.00	0.00	0.00	0.03	0.00	0.96	0.01	0.00	0.00	0.00
	Downstairs	0.00	0.00	0.00	0.00	0.00	0.00	0.00	0.00	0.13	0.00	0.01	0.86	0.00	0.00	0.00
	ClimbW	0.00	0.00	0.01	0.01	0.00	0.00	0.00	0.00	0.00	0.00	0.00	0.00	0.00	0.97	0.01
	GDownstairsW	0.00	0.00	0.00	0.00	0.01	0.00	0.00	0.00	0.00	0.00	0.00	0.00	0.03	0.96	0.96

**Figure 6.** Confusion matrix of the proposed ANN model using EMG and IMU data

**Table 2.** Class report of the proposed ANN model using EMG and IMU data

	Precision	Recall	F1 Score
<b>AdjustJacks</b>	0.91	0.95	0.93
<b>CCrossbars</b>	0.94	0.96	0.95
<b>CJacks</b>	0.97	0.98	0.97
<b>CPlank</b>	0.95	0.93	0.94
<b>CScaffold</b>	0.96	0.95	0.96
<b>DragPlank</b>	0.93	0.96	0.94
<b>Hammering</b>	0.99	0.95	0.97
<b>InsertJack</b>	0.94	0.94	0.94
<b>LiftPlank</b>	0.96	0.97	0.97
<b>Walk</b>	0.87	0.93	0.9
<b>Wrenching</b>	0.95	0.97	0.96
<b>Climb</b>	0.96	0.96	0.96
<b>Downstairs</b>	0.86	0.89	0.87
<b>ClimbW</b>	0.97	0.93	0.95
<b>GDownstairsW</b>	0.96	0.97	0.96
<b>Accuracy</b>			0.94
<b>Weighted Average</b>	0.94	0.95	0.94

#### 4.5. Real-Time Evaluation

The prediction was performed on the dataset collected from a new individual (seventh participant) to evaluate the model's robustness. The seventh participant's evaluation has been

674 performed using the trained weights of ANN generated from LOSO cross-validation. The data was  
675 not used either in training or testing the model. The dataset consists of 15,850 samples and fifteen  
676 activities. During the seventh participant experiment session, the video recorded was reviewed for  
677 activity sequence and actual class labeling to build the benchmark activities for performance  
678 evaluation by matching the time stamp in video and sensor data. Figure 7 shows the confusion  
679 matrix of the proposed ANN model on the new dataset. From the confusion matrix, it can be  
680 observed the "Downstairs" (0.27) activity was highly misclassified, followed by "GDownstairsW"  
681 (0.15), "CScaffold" (0.09), and "CJacks" (0.08). The highest misclassification of "Downstairs" was  
682 observed with the "Walk" activity. Whereas the highest classification was observed in  
683 "Wrenching" (0.98) followed by "Hammering" (0.94), "LiftPlank" (0.93), and "ClimbW" (0.91).  
684 Table 3 shows the precision, recall, and F1 score results of the ANN model on an unknown dataset.  
685 The highest precision of 0.96 was observed in the "CJacks," "Wrenching," and "Climb" activities,  
686 followed by "Hammering" (0.95), "CPlank" (0.91), and "CScaffold" (0.90). Whereas, the highest  
687 recall value of 0.98 was observed in "Wrenching" followed by "Hammering" (0.94) and  
688 "LiftPlank" (0.93). The lowest recall value was observed in "Downstairs" (0.64). The F1 score was  
689 highest in "Wrenching" (0.97) activity followed by "Hammering" (0.94), "Climb" (0.92), and  
690 "CJacks" (0.91). Overall, the prediction accuracy of the proposed ANN model on an unknown  
691 dataset is 86.87% with weighted average precision (0.86), recall (0.87), and F1 Score (0.86).  
692 Moreover, Figure 8 shows the predicted and actual sequence of activities performed by the seventh  
693 participant. The proposed model recognized the activities' sequence with the highest errors in  
694 "AdjustJacks" and "Walk" activities. Also, the time ratio difference between actual and predicted  
695 classes range between 1% to 2%, as shown in Figure 9.

True Labels	AdjustJacks	CCrossbars	CJacks	CPlank	CScaffold	DragPlank	Hammering	InsertJack	LiftPlank	Walk	Wrenching	Climb	Downstairs	ClimbW	GDownstairsW
Predicted Labels	AdjustJacks	0.85	0.00	0.00	0.00	0.04	0.04	0.04	0.02	0.00	0.01	0.00	0.00	0.00	0.00
AdjustJacks	0.00	0.88	0.00	0.02	0.00	0.02	0.00	0.07	0.01	0.00	0.00	0.00	0.00	0.00	0.00
CCrossbars	0.00	0.02	0.87	0.01	0.00	0.01	0.00	0.00	0.01	0.00	0.00	0.00	0.00	0.08	0.01
CJacks	0.00	0.05	0.00	0.87	0.06	0.00	0.00	0.00	0.00	0.00	0.00	0.00	0.00	0.00	0.00
CPlank	0.00	0.03	0.00	0.00	0.88	0.00	0.00	0.00	0.00	0.00	0.00	0.00	0.00	0.00	0.09
CScaffold	0.05	0.01	0.00	0.00	0.01	0.84	0.01	0.07	0.01	0.00	0.00	0.00	0.00	0.00	0.01
DragPlank	0.05	0.00	0.00	0.00	0.00	0.00	0.94	0.00	0.01	0.00	0.00	0.00	0.00	0.00	0.00
Hammering	0.05	0.00	0.00	0.00	0.00	0.00	0.00	0.94	0.00	0.01	0.00	0.00	0.00	0.00	0.00
InsertJack	0.05	0.00	0.00	0.00	0.00	0.00	0.02	0.88	0.03	0.00	0.01	0.00	0.00	0.00	0.00
LiftPlank	0.00	0.00	0.00	0.00	0.00	0.00	0.00	0.03	0.93	0.03	0.00	0.01	0.01	0.00	0.00
Walk	0.03	0.00	0.00	0.00	0.00	0.01	0.00	0.01	0.02	0.89	0.00	0.03	0.03	0.00	0.00
Wrenching	0.00	0.00	0.00	0.00	0.00	0.00	0.00	0.00	0.02	0.00	0.98	0.00	0.00	0.00	0.00
Climb	0.00	0.00	0.00	0.00	0.00	0.00	0.00	0.00	0.00	0.09	0.00	0.87	0.03	0.00	0.00
Downstairs	0.00	0.00	0.00	0.00	0.00	0.01	0.00	0.02	0.01	0.27	0.00	0.05	0.64	0.00	0.00
ClimbW	0.00	0.01	0.02	0.02	0.01	0.00	0.00	0.00	0.00	0.00	0.00	0.00	0.00	0.91	0.02
GDownstairsW	0.00	0.01	0.01	0.01	0.02	0.01	0.00	0.00	0.00	0.00	0.00	0.00	0.15	0.80	0.80

696

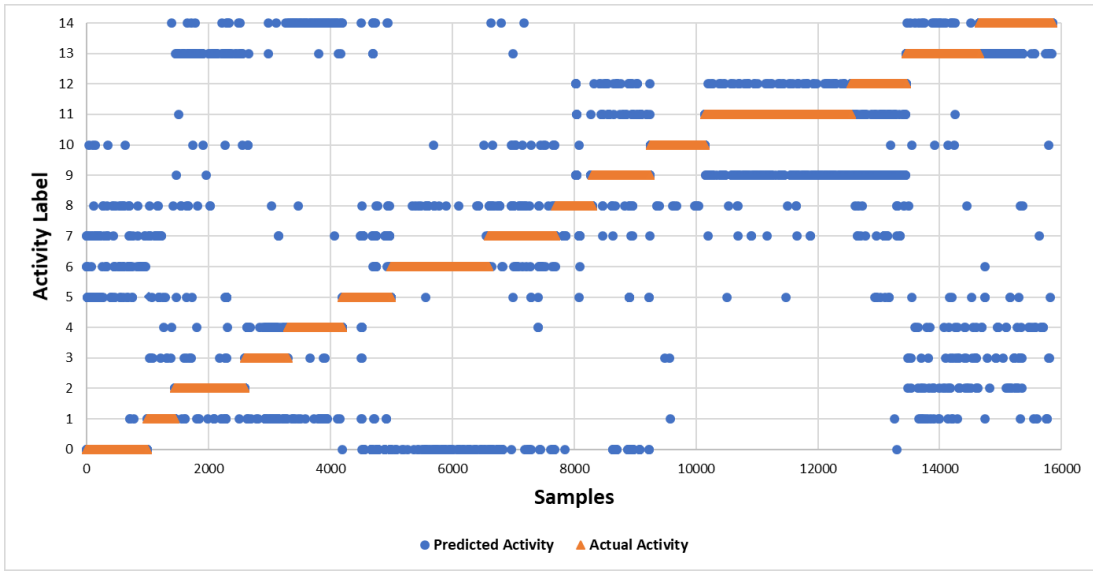
697

**Figure 7.** Confusion matrix of the proposed ANN model on the unknown dataset

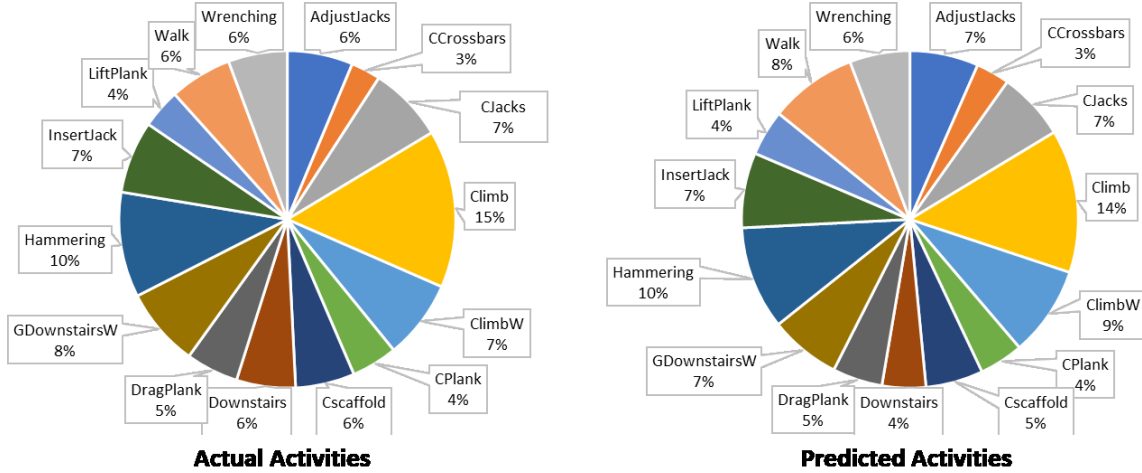
698

**Table 3.** Class report of the proposed ANN model for the unknown dataset

	Precision	Recall	F1 Score	Support
<b>AdjustJacks</b>	0.82	0.85	0.83	1000
<b>CCrossbars</b>	0.78	0.88	0.83	450
<b>CJacks</b>	0.96	0.87	0.91	1150
<b>CPlank</b>	0.91	0.87	0.89	700
<b>CScaffold</b>	0.90	0.88	0.89	900
<b>DragPlank</b>	0.88	0.84	0.86	800
<b>Hammering</b>	0.95	0.94	0.94	1600
<b>InsertJack</b>	0.84	0.88	0.86	1100
<b>LiftPlank</b>	0.80	0.93	0.86	600
<b>Walk</b>	0.63	0.89	0.74	950
<b>Wrenching</b>	0.96	0.98	0.97	900
<b>Climb</b>	0.96	0.87	0.92	2400
<b>Downstairs</b>	0.86	0.64	0.73	900
<b>ClimbW</b>	0.80	0.91	0.85	1200
<b>GDownstairsW</b>	0.88	0.80	0.84	1200
<b>Accuracy</b>	0.87	0.87	0.87	0.87
<b>Macro Average</b>	0.86	0.87	0.86	15850
<b>Weighted Average</b>	0.88	0.87	0.87	15850



699  
700 **Figure 8.** Performance of proposed ANN model on the unknown dataset – A plot showing  
701 predicted and actual classes over the entire session  
702

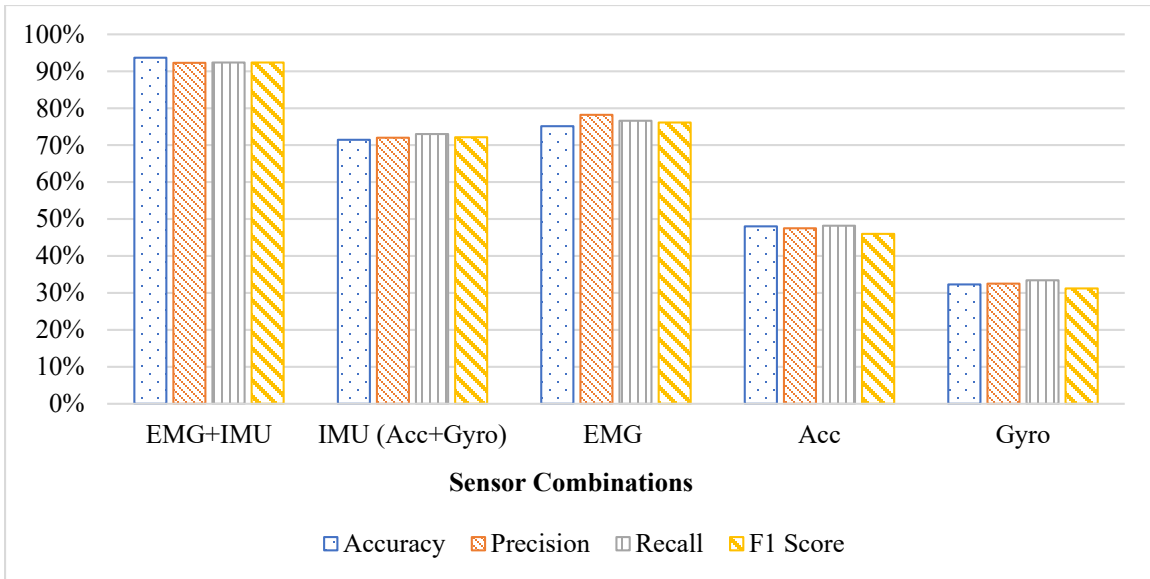


703  
704 **Figure 9.** Time ratio of actual and predicted activities  
705

#### 4.6. Comparison of Activity Recognition Performance for Different Sensor Combination

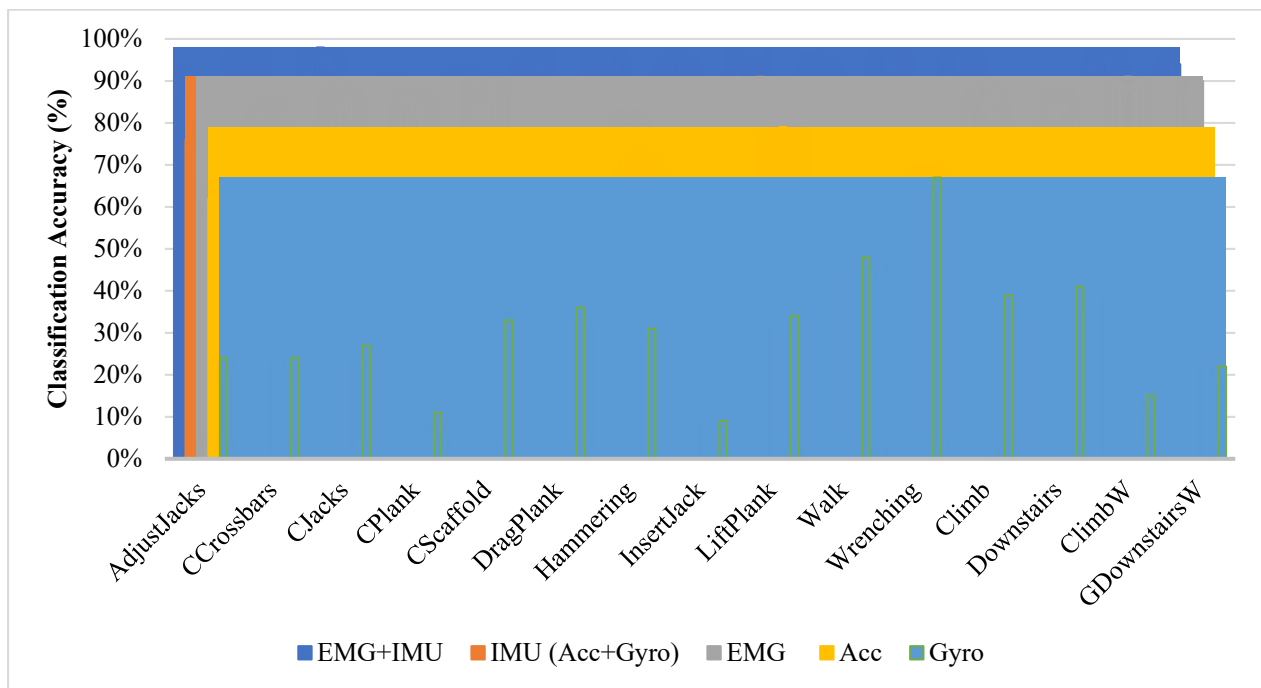
706 To understand the ANN model's performance for different sensor combinations, individual  
707 ANN models were built using various sensor combination data, namely, EMG+IMU, IMU, EMG,  
708 Acc, and Gyro. All these models were built using the framework proposed in this study, and all

709 the models were evaluated for performance and diagnosed for overfitting or underfit problems.  
710 The overall accuracy, weighted precision, weighted recall, and weighted F1 Score of each sensor  
711 combination's best performance model are presented in Figure 10. From Figure 11, it can be  
712 observed the EMG+IMU model achieved the highest accuracy of 93.68%, followed by EMG  
713 (75.12%), IMU (71.45%), Acc (48.00%), and Gyro (32.30%). From this analysis, it can be  
714 concluded that EMG+IMU data helps improve classification accuracy. Also, the sensor  
715 combination model performance was analyzed for different classes. As shown in Figure 11, the  
716 EMG+IMU model has outperformed other models in all classes. Between EMG and IMU models,  
717 EMG outperformed IMU in the majority of the activities. EMG models performed better for  
718 "CCrossbars", "CJacks", "CPlank", "CScaffold," "DragPlank", "Hammering", "InsertJack",  
719 "Walk", "Climb", "Downstairs", "ClimbW", and "GDownstairsW". Whereas, IMU models have  
720 better accuracy than EMG models for "AdjustJacks," "LiftPlank," and "Wrenching." For  
721 "Wrenching" activity, both EMG and IMU performed equally. The acceleration and gyroscope  
722 models have performed poorly compared to EMG+IMU, IMU, and EMG. Among acceleration  
723 and gyroscope, the acceleration models have better accuracy. From Figure 10 and Figure 11, it can  
724 be concluded that EMG+IMU features yield higher accuracy for all the classes compared to other  
725 sensor combinations.



726

727 **Figure 10.** Comparison of classification performance of the ANN model using different sensor  
 728 combination



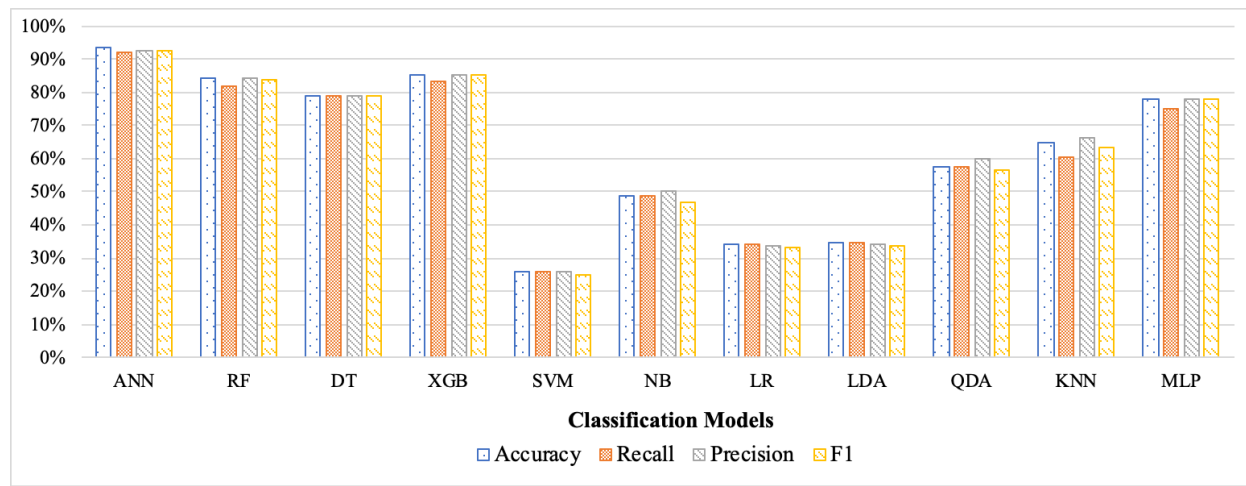
729

730 **Figure 11.** Comparison of classification performance of the ANN model for all activities for  
 731 different sensor data

732

733 **4.7. Comparison of Proposed Model with other Classification Models**

734 It is essential to determine how well the proposed ANN model performs compared to other  
735 classification algorithms. Therefore, the EMG+IMU dataset was further used to test with other  
736 existing classification models such as Random Forest (RF), Decision Trees (DT), Gradient  
737 Boosting (XGB), Support Vector Machine (SVM), Naïve Bayes (NB), Logistic Regression (LR),  
738 Linear Discriminant Analysis (LDA), Quadratic Discriminant Analysis (QDA), K-nearest  
739 Neighbors (KNN), and Multilayer Perceptron (MLP). Leave One Subject Out cross-validation  
740 technique was used to evaluate all the classifiers' performance with six-folds. Figure 12 compares  
741 the cross-validation accuracy of all the classification algorithms on the EMG+IMU dataset. It can  
742 be observed that the highest accuracy was obtained using the proposed ANN (93.68%) model,  
743 followed by XGB (85.45%), RF (84.10%), and DT (79.11%). Whereas the least accuracy was  
744 obtained in the SVM classifier case with 0.26, 0.25, and 0.24 recall, precision, and F1 Score,  
745 respectively.



746

747 **Figure 12.** Comparison of activity recognition performance using the ANN model for  
748 different sensor data

749

750 **5. Discussion**

751 In this study, a case study of scaffold builder activities was conducted to evaluate the proposed  
752 worker activity recognition framework's performance using forearm EMG and IMU data from the  
753 dominant hand. The use of armband sensors on the dominant hand can recognize whole-body  
754 activities highly suitable for construction applications. The case study results show that the ANN  
755 model developed using EMG and IMU has achieved the highest average classification accuracy  
756 of 93.29% for all fifteen activities. Since the construction activities involve either muscle activity  
757 and body movement, the use of EMG and IMU helps in recognizing complex construction  
758 activities involving different motions and body parts. From the results of the current case study,  
759 the activities involving motion such as adjusting jacks, dragging plank, lifting plank, walking,  
760 wrenching, and hammering, IMU data model have shown better accuracy compared to EMG  
761 model. Whereas in the case of activities involving muscle activity or material handling such as  
762 carrying scaffold, carrying plank, carrying jack, and carrying tool bag, the EMG data model has  
763 higher accuracy than the IMU data model. These results conclude that the proposed framework  
764 can recognize activities that do not involve considerable body movement of human body parts or  
765 repetitive activities, which is one of the significant challenges of previous activity recognition  
766 models [13]. Besides, the proposed framework can recognize a more significant number of  
767 activities compared to previous models. The high precision, recall, and F1 Score of the proposed  
768 model on real-time predictions show that the model can be used for real-time worker activity  
769 monitoring for safety, productivity, and project controls applications.

770 One of the common issues with deep learning models is the necessity of large datasets, and  
771 this issue is addressed by incorporating a data augmentation technique in the framework. The data  
772 augmentation trains better, as seen in learning curves, and helps model generalization and removes

773 human variabilities. As previous studies stated [6], the sensor data fusion at a lower-level (signal  
774 level) improved accuracy significantly by eliminating the redundancy and considering  
775 dependencies and correlation between different features. The signal-level data fusion improved  
776 the accuracy and eliminates the process of extracting features from the raw data, which requires  
777 domain knowledge. Besides, the hyperparameter optimization using Bayesian TPE automates  
778 network parameter selection, which helps in adopting the proposed framework for any construction  
779 activity recognition and prevents human errors. Since the proposed framework is fully automated  
780 and independent of activities, it can be extended to any trade or multiple trades by retraining the  
781 model with new activity data.

782 **6. Limitations and Future Work**

783 Test Subjects: As this study was initially designed to investigate the testbed before actual  
784 production on large-scale workers in a real-world environment, the experiment was performed  
785 with limited non-construction workers in a semi-construction environment. Since the proposed  
786 framework is independent of human variability and environment, retraining the model with data  
787 from construction workers enables producing large-scale and field-ready models.

788 Future Work: We further expect to understand how the armband sensor position (slid or  
789 rotated) on the forearm influences the activity recognition results. Even though the signal-level  
790 sensor data fusion yielded high accuracies, we want to investigate how other data fusion levels  
791 (feature-level and decision-level) will affect the activity recognition performance. The authors plan  
792 to develop one generic model to recognize multiple construction trades' activities using the  
793 proposed framework. Future research investigates the performance of recurrent neural networks  
794 such as long short-term memory (LSTM) for construction activity recognition.

795

796 **7. Conclusions**

797 This study proposes an automated construction worker activity recognition method using  
798 forearm EMG and IMU data. The proposed framework is fully automated and can be applied for  
799 any number of activities and different construction trades by retraining the model with additional  
800 training data. Moreover, data augmentation and hyperparameter optimization help achieve high  
801 accuracy with limited participant data. The proposed method was validated and evaluated through  
802 a case study on scaffold builder activities, including complex construction activities involving  
803 different body parts (wrist, forearm, upper body, lower body, and whole-body) and various  
804 motions (repetitive motion, impulsive motion, and free motion). The proposed ANN model was  
805 able to classify fifteen scaffold builder activities with an overall testing accuracy of 93.29% and  
806 real-time prediction accuracy of 87%. The sequences and time ratio plots showed that the model  
807 could successfully predict the sequence and time spent on each activity with minimal error. The  
808 performance evaluation of the ANN model on different sensor combinations showed that the  
809 classification accuracy was highest for EMG+IMU (93.29%), followed by EMG alone (75.1%)  
810 alone and IMU (71.4%) alone. The results also show that the EMG data alone performed better  
811 than IMU data alone and acceleration data alone for carrying scaffold, carrying plank, carrying  
812 crossbars, inserting jacks, and climbing stairs with weight. In contrast, the IMU data alone  
813 performed better than EMG data alone for the rest of the activities. Since most construction  
814 activities involve motion and muscle activity, EMG and IMU data have increased the accuracy of  
815 activity recognition. The proposed model was also compared with the other machine learning-  
816 based classification algorithms, and the comparisons show that the proposed model outperformed  
817 all the other classifiers.

818      Compared to previous studies, the main advantages of the proposed worker activity recognition  
819      system are inexpensive equipment cost, fully automated framework, low computation cost, ability  
820      to recognize complex construction activities, and recognizing more activities. Since the proposed  
821      framework is fully automated, scalable, robust, and adaptable, the system can be  
822      commercialized. As the future direction, we will further explore the feasibility of workload  
823      assessment, fatigue monitoring, and productivity assessment using the proposed system and  
824      methodology.

825

## 826      **Acknowledgement**

827      This material is based upon work supported by the National Science Foundation under Grant No.  
828      #2026575. Any opinions, findings, and conclusions or recommendations expressed in this material  
829      are those of the author(s) and do not necessarily reflect the views of the National Science  
830      Foundation.

## 831      **References**

832      [1]      R.d.      Best,      U.S.      Construction      Industry      -      Statistics      &      Facts,  
833      2020.<https://www.statista.com/topics/974/construction/>, (January 12 2021)

834      [2]      S. Kim, S. Chang, D. Castro-Lacouture, Dynamic modeling for analyzing impacts of  
835      skilled labor shortage on construction project management, Journal of Management in  
836      Engineering 36 (1) (2020) 04019035

837      [3]      B.Y. Future, Craft Labor Demand, 2020, (July 5th 2020)

838      [4]      H. Karimi, T.R. Taylor, P.M. Goodrum, C. Srinivasan, Quantitative analysis of the impact  
839      of craft worker availability on construction project safety performance, Construction  
840      innovation (2016)

841 [5] O.A. Ayodele, A. Chang-Richards, V. González, Factors affecting workforce turnover in  
842 the construction sector: a systematic review, *Journal of Construction Engineering and*  
843 *Management* 146 (2) (2020) 03119010

844 [6] C.R. Ahn, S. Lee, C. Sun, H. Jebelli, K. Yang, B. Choi, Wearable sensing technology  
845 applications in construction safety and health, *Journal of Construction Engineering and*  
846 *Management* 145 (11) (2019) 03119007

847 [7] I. Awolusi, E. Marks, M. Hallowell, Wearable technology for personalized construction  
848 safety monitoring and trending: Review of applicable devices, *Automation in construction*  
849 85 (2018) 96-106

850 [8] A. Aryal, A. Ghahramani, B. Becerik-Gerber, Monitoring fatigue in construction workers  
851 using physiological measurements, *Automation in construction* 82 (2017) 154-165

852 [9] J. Häikiö, J. Kallio, S.-M. Mäkelä, J. Keränen, IoT-based safety monitoring from the  
853 perspective of construction site workers, *International Journal of Occupational and*  
854 *Environmental Safety* 4 (1) (2020) 1-14

855 [10] S. Hwang, H. Jebelli, B. Choi, M. Choi, S. Lee, Measuring workers' emotional state during  
856 construction tasks using wearable EEG, *Journal of Construction Engineering and*  
857 *Management* 144 (7) (2018) 04018050

858 [11] H. Luo, C. Xiong, W. Fang, P.E. Love, B. Zhang, X. Ouyang, Convolutional neural  
859 networks: Computer vision-based workforce activity assessment in construction,  
860 *Automation in construction* 94 (2018) 282-289

861 [12] D. Roberts, M. Golparvar-Fard, End-to-end vision-based detection, tracking and activity  
862 analysis of earthmoving equipment filmed at ground level, *Automation in construction* 105  
863 (2019) 102811

864 [13] B. Sherafat, C.R. Ahn, R. Akhavian, A.H. Behzadan, M. Golparvar-Fard, H. Kim, Y.-C.  
865 Lee, A. Rashidi, E.R. Azar, Automated Methods for Activity Recognition of Construction  
866 Workers and Equipment: State-of-the-Art Review, *Journal of Construction Engineering  
867 and Management* 146 (6) (2020) 03120002

868 [14] P. Chan, A. Kaka, Construction productivity measurement: A comparison of two case  
869 studies, 20th Annual ARCOM Conference, Edinburgh, Scotland, 2004

870 [15] C.-F. Cheng, A. Rashidi, M.A. Davenport, D.V. Anderson, C. Sabillon, Software and  
871 hardware requirements for audio-based analysis of construction operations, Reston, VA:  
872 ASCE, 2018

873 [16] L. Joshua, K. Varghese, Accelerometer-based activity recognition in construction, *Journal  
874 of computing in civil engineering* 25 (5) (2011) 370-379

875 [17] D. Wang, J. Chen, D. Zhao, F. Dai, C. Zheng, X. Wu, Monitoring workers' attention and  
876 vigilance in construction activities through a wireless and wearable  
877 electroencephalography system, *Automation in construction* 82 (2017) 122-137

878 [18] J. Ryu, J. Seo, H. Jebelli, S. Lee, Automated action recognition using an accelerometer-  
879 embedded wristband-type activity tracker, *Journal of Construction Engineering and  
880 Management* 145 (1) (2019) 04018114

881 [19] Z. Yang, Y. Yuan, M. Zhang, X. Zhao, B. Tian, Assessment of construction workers' labor  
882 intensity based on wearable smartphone system, *Journal of Construction Engineering and  
883 Management* 145 (7) (2019) 04019039

884 [20] R. Akhavian, A.H. Behzadan, Coupling human activity recognition and wearable sensors  
885 for data-driven construction simulation, *ITcon* 23 (2018) 1-15

886 [21] J. Yang, Z. Shi, Z. Wu, Vision-based action recognition of construction workers using  
887 dense trajectories, *Advanced Engineering Informatics* 30 (3) (2016) 327-336

888 [22] A. Albert, M.R. Hallowell, B. Kleiner, A. Chen, M. Golparvar-Fard, Enhancing  
889 construction hazard recognition with high-fidelity augmented virtuality, *Journal of*  
890 *Construction Engineering and Management* 140 (7) (2014) 04014024

891 [23] A. Khosrowpour, I. Fedorov, A. Holynski, J.C. Niebles, M. Golparvar-Fard, Automated  
892 worker activity analysis in indoor environments for direct-work rate improvement from  
893 long sequences of RGB-D images, *Construction Research Congress 2014: Construction*  
894 *in a Global Network*, 2014, pp. 729-738

895 [24] G. Cezar, Activity recognition in construction sites using 3D accelerometer and gyrometer,  
896 Accessed Octobar 10 (2012) 2018

897 [25] S.H. Khan, M. Sohail, Activity monitoring of workers using single wearable inertial sensor,  
898 2013 International Conference on Open Source Systems and Technologies, IEEE, 2013,  
899 pp. 60-67

900 [26] L. Joshua, K. Varghese, Selection of accelerometer location on bricklayers using decision  
901 trees, *Computer-Aided Civil and Infrastructure Engineering* 28 (5) (2013) 372-388

902 [27] K. Yang, S. Aria, C.R. Ahn, T.L. Stentz, Automated detection of near-miss fall incidents  
903 in iron workers using inertial measurement units, *Construction Research Congress 2014:*  
904 *Construction in a Global Network*, 2014, pp. 935-944

905 [28] T.-K. Lim, S.-M. Park, H.-C. Lee, D.-E. Lee, Artificial neural network-based slip-trip  
906 classifier using smart sensor for construction workplace, *Journal of Construction*  
907 *Engineering and Management* 142 (2) (2016) 04015065

908 [29] R. Akhavian, A.H. Behzadan, Smartphone-based construction workers' activity  
909 recognition and classification, Automation in construction 71 (2016) 198-209

910 [30] T. Zhang, Y.-C. Lee, M. Scarpiniti, A. Uncini, A supervised machine learning-based sound  
911 identification for construction activity monitoring and performance evaluation,  
912 Construction Research Congress 2018, 2018, pp. 358-366

913 [31] S. Deb, D.W. Carruth, R. Sween, L. Strawderman, T.M. Garrison, Efficacy of virtual  
914 reality in pedestrian safety research, Appl Ergon 65 (2017) 449-460.'doi':  
915 10.1016/j.apergo.2017.03.007

916 [32] J. Bosch, N. Gracias, P. Ridao, D. Ribas, Omnidirectional underwater camera design and  
917 calibration, Sensors (Basel) 15 (3) (2015) 6033-6065.'doi': 10.3390/s150306033

918 [33] P. Vepakomma, D. De, S.K. Das, S. Bhansali, A-Wristocracy: Deep learning on wrist-  
919 worn sensing for recognition of user complex activities, 2015 IEEE 12th International  
920 conference on wearable and implantable body sensor networks (BSN), IEEE, 2015, pp. 1-  
921 6

922 [34] D. Cook, K.D. Feuz, N.C. Krishnan, Transfer Learning for Activity Recognition: A Survey,  
923 Knowl Inf Syst 36 (3) (2013) 537-556.'doi': 10.1007/s10115-013-0665-3

924 [35] J. Wang, Y. Chen, S. Hao, X. Peng, L. Hu, Deep learning for sensor-based activity  
925 recognition: A survey, Pattern Recognition Letters 119 (2019) 3-11

926 [36] O.D. Lara, M.A. Labrador, A survey on human activity recognition using wearable sensors,  
927 IEEE communications surveys & tutorials 15 (3) (2012) 1192-1209

928 [37] E. Munguia Tapia, Using machine learning for real-time activity recognition and  
929 estimation of energy expenditure, Massachusetts Institute of Technology, 2008

930 [38] K. Chen, D. Zhang, L. Yao, B. Guo, Z. Yu, Y. Liu, Deep learning for sensor-based human  
931 activity recognition: overview, challenges and opportunities, arXiv preprint  
932 arXiv:2001.07416 (2020)

933 [39] Y. Bengio, Deep learning of representations: Looking forward, International Conference  
934 on Statistical Language and Speech Processing, Springer, 2013, pp. 1-37

935 [40] K.M. Rashid, J. Louis, Times-series data augmentation and deep learning for construction  
936 equipment activity recognition, Advanced Engineering Informatics 42 (2019) 100944

937 [41] H. Lee, C.R. Ahn, N. Choi, T. Kim, H. Lee, The effects of housing environments on the  
938 performance of activity-recognition systems using Wi-Fi channel state information: An  
939 exploratory study, Sensors 19 (5) (2019) 983

940 [42] J.A. Álvarez-García, P. Barsocchi, S. Chessa, D. Salvi, Evaluation of localization and  
941 activity recognition systems for ambient assisted living: The experience of the 2012  
942 EvAAL competition, Journal of Ambient Intelligence and Smart Environments 5 (1)  
943 (2013) 119-132

944 [43] F.J. Ordonez, D. Roggen, Deep Convolutional and LSTM Recurrent Neural Networks for  
945 Multimodal Wearable Activity Recognition, Sensors (Basel) 16 (1) (2016) 115.'doi':  
946 10.3390/s16010115

947 [44] R. Khusainov, D. Azzi, I.E. Achumba, S.D. Bersch, Real-time human ambulation, activity,  
948 and physiological monitoring: taxonomy of issues, techniques, applications, challenges and  
949 limitations, Sensors (Basel) 13 (10) (2013) 12852-12902.'doi': 10.3390/s131012852

950 [45] S. Kim, M.A. Nussbaum, Performance evaluation of a wearable inertial motion capture  
951 system for capturing physical exposures during manual material handling tasks,  
952 Ergonomics 56 (2) (2013) 314-326.'doi': 10.1080/00140139.2012.742932

953 [46] T. Seel, J. Raisch, T. Schauer, IMU-based joint angle measurement for gait analysis,  
954 Sensors (Basel) 14 (4) (2014) 6891-6909.'doi': 10.3390/s140406891

955 [47] A. Alwasel, E.M. Abdel-Rahman, C.T. Haas, S. Lee, Experience, productivity, and  
956 musculoskeletal injury among masonry workers, Journal of Construction Engineering and  
957 Management 143 (6) (2017) 05017003

958 [48] J. Chen, J. Qiu, C. Ahn, Construction worker's awkward posture recognition through  
959 supervised motion tensor decomposition, Automation in construction 77 (2017) 67-81

960 [49] N.D. Nath, R. Akhavian, A.H. Behzadan, Ergonomic analysis of construction worker's  
961 body postures using wearable mobile sensors, Applied ergonomics 62 (2017) 107-117

962 [50] T.-K. Lim, S.-M. Park, H.-C. Lee, D.-E. Lee, Artificial neural network-based slip-trip  
963 classifier using smart sensor for construction workplace, Journal of Construction  
964 Engineering and Management 142 (2) (2015) 04015065

965 [51] K. Yang, C.R. Ahn, M.C. Vuran, S.S. Aria, Semi-supervised near-miss fall detection for  
966 ironworkers with a wearable inertial measurement unit, Automation in construction 68  
967 (2016) 194-202

968 [52] W. Wu, H. Yang, D.A. Chew, S.-h. Yang, A.G. Gibb, Q. Li, Towards an autonomous real-  
969 time tracking system of near-miss accidents on construction sites, Automation in  
970 construction 19 (2) (2010) 134-141

971 [53] S. Hwang, J. Seo, H. Jebelli, S. Lee, Feasibility analysis of heart rate monitoring of  
972 construction workers using a photoplethysmography (PPG) sensor embedded in a  
973 wristband-type activity tracker, Automation in construction 71 (2016) 372-381

974 [54] H. Jebelli, B. Choi, H. Kim, S. Lee, Feasibility study of a wristband-type wearable sensor  
975 to understand construction workers' physical and mental status, Construction Research  
976 Congress, 2018, pp. 367-377

977 [55] A.D. Nimbarde, F. Aghazadeh, L.H. Ikuma, C.M. Harvey, Neck disorders among  
978 construction workers: understanding the physical loads on the cervical spine during static  
979 lifting tasks, Industrial health 48 (2) (2010) 145-153

980 [56] T.S. Abdelhamid, J.G. Everett, Physiological demands during construction work, Journal  
981 of Construction Engineering and Management 128 (5) (2002) 427-437

982 [57] F.L. Chang, Y.M. Sun, K.H. Chuang, D.J. Hsu, Work fatigue and physiological symptoms  
983 in different occupations of high-elevation construction workers, Appl Ergon 40 (4) (2009)  
984 591-596.'doi': 10.1016/j.apergo.2008.04.017

985 [58] Z.S. Maman, M.A.A. Yazdi, L.A. Cavuoto, F.M. Megahed, A data-driven approach to  
986 modeling physical fatigue in the workplace using wearable sensors, Applied ergonomics  
987 65 (2017) 515-529

988 [59] S. Hasanzadeh, B. Esmaeili, M.D. Dodd, Measuring the impacts of safety knowledge on  
989 construction workers' attentional allocation and hazard detection using remote eye-  
990 tracking technology, Journal of Management in Engineering 33 (5) (2017) 04017024

991 [60] I. Jeelani, K. Han, A. Albert, Automating and scaling personalized safety training using  
992 eye-tracking data, Automation in construction 93 (2018) 63-77

993 [61] H. Jebelli, S. Lee, Feasibility of Wearable Electromyography (EMG) to Assess  
994 Construction Workers' Muscle Fatigue, Advances in Informatics and Computing in Civil  
995 and Construction Engineering, Springer, 2019, pp. 181-187.'doi':

996 [62] H. Jebelli, M.M. Khalili, S. Lee, Mobile EEG-based workers' stress recognition by  
997 applying deep neural network, *Advances in Informatics and Computing in Civil and*  
998 *Construction Engineering*, Springer, 2019, pp. 173-180.'doi':

999 [63] J. Gong, C.H. Caldas, An intelligent video computing method for automated productivity  
1000 analysis of cyclic construction operations, *Computing in Civil Engineering* (2009), 2009,  
1001 pp. 64-73.'doi':

1002 [64] C. Kim, T. Park, H. Lim, H. Kim, On-site construction management using mobile  
1003 computing technology, *Automation in construction* 35 (2013) 415-423

1004 [65] L. Joshua, K. Varghese, Accelerometer-based activity recognition in construction, *Journal*  
1005 *of computing in civil engineering* 25 (5) (2010) 370-379

1006 [66] L. Joshua, K. Varghese, Automated recognition of construction labour activity using  
1007 accelerometers in field situations, *International Journal of Productivity and Performance*  
1008 *Management* 63 (7) (2014) 841-862

1009 [67] J. Ryu, J. Seo, H. Jebelli, S. Lee, Automated action recognition using an accelerometer-  
1010 embedded wristband-type activity tracker, *Journal of Construction Engineering and*  
1011 *Management* 145 (1) (2018) 04018114

1012 [68] T. Cheng, J. Teizer, G.C. Migliaccio, U.C. Gatti, Automated task-level activity analysis  
1013 through fusion of real time location sensors and worker's thoracic posture data, *Automation*  
1014 *in construction* 29 (2013) 24-39

1015 [69] N.D. Nath, T. Chaspéri, A.H. Behzadan, Automated ergonomic risk monitoring using  
1016 body-mounted sensors and machine learning, *Advanced Engineering Informatics* 38  
1017 (2018) 514-526

1018 [70] L. Bao, S.S. Intille, Activity recognition from user-annotated acceleration data,  
1019 International conference on pervasive computing, Springer, 2004, pp. 1-17

1020 [71] C.C. Yang, Y.L. Hsu, A review of accelerometry-based wearable motion detectors for  
1021 physical activity monitoring, Sensors (Basel) 10 (8) (2010) 7772-7788.'doi':  
1022 10.3390/s100807772

1023 [72] N. Ravi, N. Dandekar, P. Mysore, M.L. Littman, Activity recognition from accelerometer  
1024 data, Aaai, Vol. 5, 2005, pp. 1541-1546

1025 [73] S. Chernbumroong, A.S. Atkins, H. Yu, Activity classification using a single wrist-worn  
1026 accelerometer, 2011 5th International Conference on Software, Knowledge Information,  
1027 Industrial Management and Applications (SKIMA) Proceedings, IEEE, 2011, pp. 1-6

1028 [74] M. Shoaib, S. Bosch, O. Incel, H. Scholten, P. Havinga, Complex human activity  
1029 recognition using smartphone and wrist-worn motion sensors, Sensors 16 (4) (2016) 426

1030 [75] R. Akhavian, A.H. Behzadan, Productivity analysis of construction worker activities using  
1031 smartphone sensors, Proc., 16th Int. Conf. Comput. Civil Building Eng, 2016

1032 [76] A. Bayat, M. Pomplun, D.A. Tran, A study on human activity recognition using  
1033 accelerometer data from smartphones, Procedia Computer Science 34 (2014) 450-457

1034 [77] J.R. Kwapisz, G.M. Weiss, S.A. Moore, Activity recognition using cell phone  
1035 accelerometers, ACM SigKDD Explorations Newsletter 12 (2) (2011) 74-82

1036 [78] S.S. Intille, L. Bao, E.M. Tapia, J. Rondoni, Acquiring in situ training data for context-  
1037 aware ubiquitous computing applications, Proceedings of the SIGCHI conference on  
1038 Human factors in computing systems, 2004, pp. 1-8

1039 [79] J. Yang, Toward physical activity diary: motion recognition using simple acceleration  
1040 features with mobile phones, Proceedings of the 1st international workshop on Interactive  
1041 multimedia for consumer electronics, ACM, 2009, pp. 1-10

1042 [80] M.-K. Tsai, Automatically determining accidental falls in field surveying: A case study of  
1043 integrating accelerometer determination and image recognition, Safety science 66 (2014)  
1044 19-26

1045 [81] K. Yang, H. Jebelli, C. Ahn, M. Vuran, Threshold-based approach to detect near-miss falls  
1046 of iron workers using inertial measurement units, Computing in Civil Engineering 2015,  
1047 2015, pp. 148-155.'doi':

1048 [82] H. Koskimaki, V. Huikari, P. Siirtola, P. Laurinen, J. Roning, Activity recognition using a  
1049 wrist-worn inertial measurement unit: A case study for industrial assembly lines, 2009  
1050 17th Mediterranean Conference on Control and Automation, IEEE, 2009, pp. 401-405

1051 [83] O.C. Ann, L.B. Theng, Human activity recognition: a review, 2014 IEEE international  
1052 conference on control system, computing and engineering (ICCSCE 2014), IEEE, 2014,  
1053 pp. 389-393

1054 [84] Y.K. Cho, K. Kim, S. Ma, J. Ueda, A robotic wearable exoskeleton for construction  
1055 worker's safety and health, ASCE Construction Research Congress, 2018, pp. 19-28

1056 [85] M. Sathiyanarayanan, S. Rajan, MYO Armband for physiotherapy healthcare: A case study  
1057 using gesture recognition application, 2016 8th International Conference on  
1058 Communication Systems and Networks (COMSNETS), IEEE, 2016, pp. 1-6

1059 [86] R. Guérat, A. Cierro, J. Vanderdonckt, J.L. Pérez-Medina, Gesture Elicitation and Usability  
1060 Testing for an Armband Interacting with Netflix and Spotify, International Conference on  
1061 Information Technology & Systems, Springer, 2019, pp. 625-637

1062 [87] M. Shanker, M.Y. Hu, M.S. Hung, Effect of data standardization on neural network  
1063 training, *Omega* 24 (4) (1996) 385-397

1064 [88] F. Chollet, others. 2015, Keras: Deep learning library for theano and tensorflow. URL:  
1065 <https://keras.io/k> (2015)

1066 [89] L. Yang, A. Shami, On hyperparameter optimization of machine learning algorithms:  
1067 Theory and practice, *Neurocomputing* 415 (2020) 295-316

1068 [90] Z. Zhang, Improved adam optimizer for deep neural networks, 2018 IEEE/ACM 26th  
1069 International Symposium on Quality of Service (IWQoS), IEEE, 2018, pp. 1-2

1070 [91] D. Gholamiangonabadi, N. Kiselov, K. Grolinger, Deep Neural Networks for Human  
1071 Activity Recognition With Wearable Sensors: Leave-One-Subject-Out Cross-Validation  
1072 for Model Selection, *IEEE Access* 8 (2020) 133982-133994

1073 [92] OSHA, Scaffolding eTool,  
1074 2020. <https://www.osha.gov/SLTC/etools/scaffolding/index.html>, (JuKy 6th 2020)

1075 [93] K.M. Halperin, M. McCann, An evaluation of scaffold safety at construction sites, *Journal*  
1076 of safety research 35 (2) (2004) 141-150

1077 [94] J.C. Rubio-Romero, M.C.R. Gámez, J.A. Carrillo-Castrillo, Analysis of the safety  
1078 conditions of scaffolding on construction sites, *Safety science* 55 (2013) 160-164

1079